ER80115

GEOLOGICAL SURVEY EXPLANATORY REPORT

SHEET 91

DAVEY

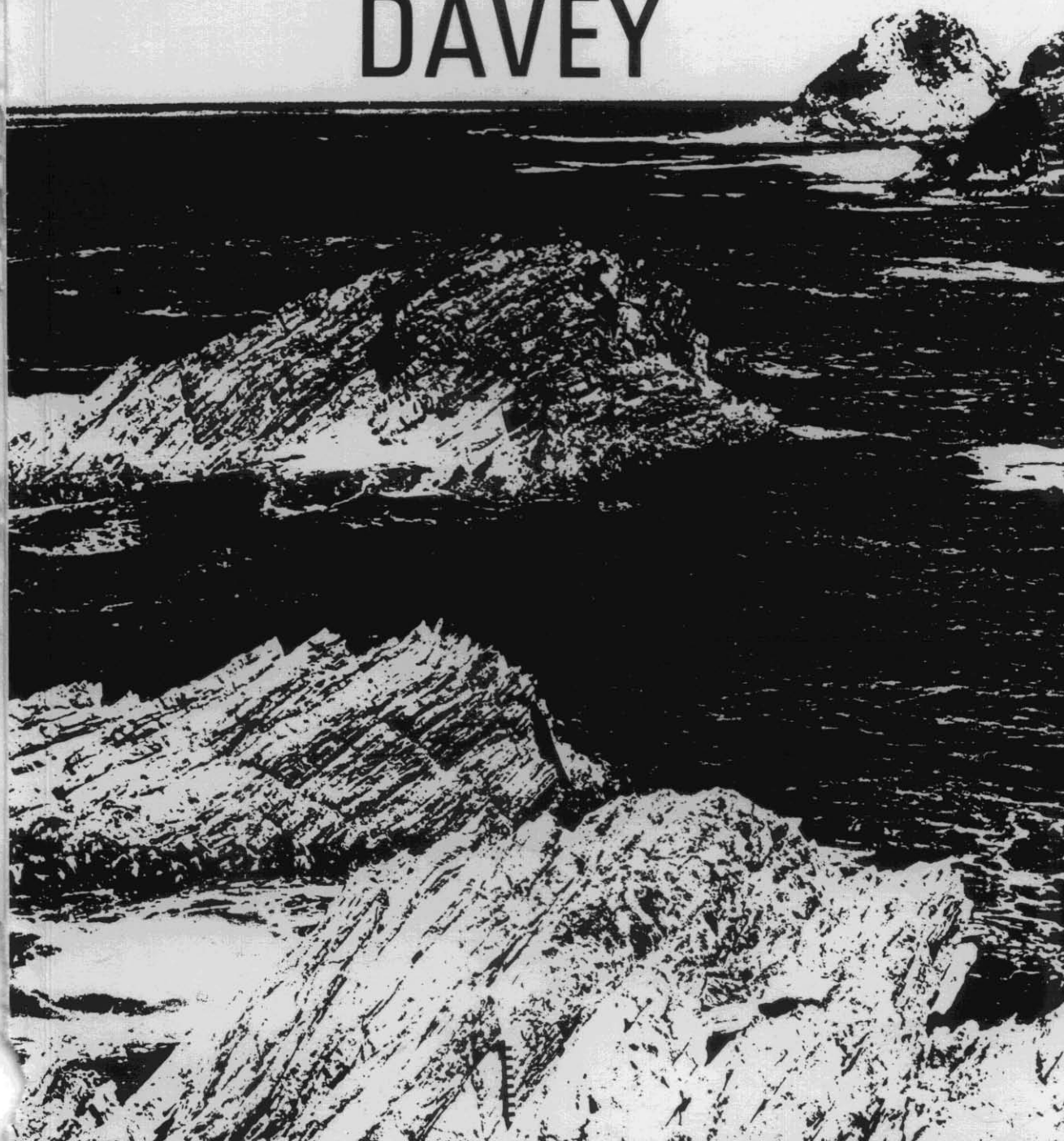

TASMANIA DEPARTMENT OF MINES

1982

GEOLOGICAL SURVEY EXPLANATORY REPORT

GEOLOGICAL ATLAS 1:50000 SERIES

ZONE 7 SHEET 91 (8011S)

DAVEY

by P.R. WILLIAMS, B.Sc.(Hons), Ph.D.

DEPARTMENT OF MINES, G.P.O. BOX 124B, HOBART, TASMANIA 7001

ISBN 0 7246 0507 X

WILLIAMS, P.R. 1982. Geological atlas 1:50 000 series. Sheet 91 (8011S). Davey. *Explan.Rep.geol.Surv.Tasm.*

ISBN 0 7246 0507 X

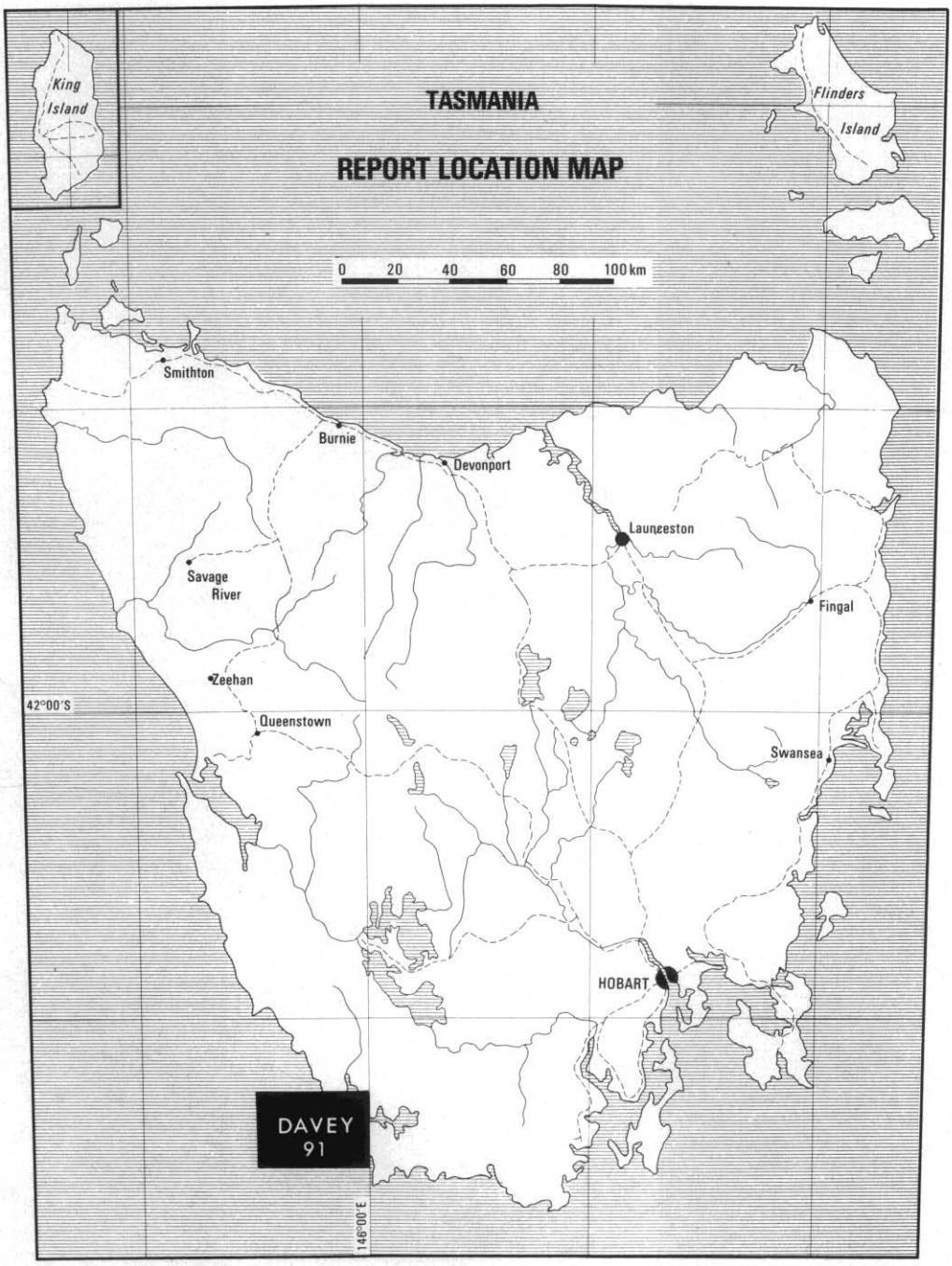

Figure 1. *Location of Davey Quadrangle.*

5 cm

CONTENTS

LIST OF FIGURES

LIST OF PLATES

INTRODUCTION

The Davey Quadrangle is situated in the far south-west of Tasmania and is bounded by latitudes 43°15'S and 43°30'S and longitudes 145°30'E and 146°E (fig. 1); it includes Port Davey and the entrance to Bathurst Channel. The whole area, including the offshore islands, is within the South-West National Park. Access is by boat or helicopter. There are no established foot tracks into the area, which is separated from the major routes in the Park by the Spring River valley.

Commercial activity in the quadrangle has been limited. Huon pine (*Dacrydium franklinii*) was cut in the Davey River, floated downstream, and shipped from Port Davey from as early as 1825 (Scott, 1876). Logging continued until the end of the last century. Activity is now restricted to fishing for crayfish and abalone, and Port Davey is used for shelter only.

The map sheet was published on a scale of 1:50 000 in 1979, after the area was mapped on a scale of 1:15 840. Previous geological activity in the quadrangle has been restricted to prospecting and reconnaissance mapping. The Broken Hill Proprietary Co. Ltd undertook reconnaissance geological mapping of the south-west region under lease in 1965 and 1966. Rock descriptions from the area have been made by Spry and Baker (1965) and Keid (1944). Stefanski (1961), Everard (1961), and Keid (1944) described sand containing heavy minerals, mainly garnet and rutile. Stefanski (1961) reported the occurrence of copper mineralisation from south of Paradise Lagoon [DN042107], but no economic mineral deposits have been located in the quadrangle.

PETROGRAPHY OF THE PRECAMBRIAN ROCKS

The rocks underlying the Davey Quadrangle are dominantly regionally metamorphosed rocks forming a south-western extension of the rocks of the Tyennan Region, which extends from Cradle Mountain to the south coast of Tasmania.

Six rock types have been delineated in the Davey Quadrangle, based upon distinctions mappable in the field. It is difficult to map these rock types away from the coast, because outcrop in pelitic units is very poor. However major units have been delineated in the Davey Head area, and these define a major paired anticline and syncline.

GARNET AMPHIBOLE EPIDOTE SCHIST AND AMPHIBOLITE (Pa)

These rocks occur in isolated, oval-shaped bodies [DN090046] or elongate sheets [DN038089], usually steeply dipping. They are dark green, medium-grained rocks with pink, spherical, porphyroblastic garnet crystals less than 2 mm in diameter. Schistose rocks have biotite and amphibole aligned in the schistosity direction. Individual amphibolite bodies are texturally and modally distinct and either the conditions of metamorphism, or their original compositions, differed. All the amphibolite bodies are surrounded by quartz, white-mica, biotite garnet schist.

West of Toogee Hill [DN038089]

This body is a layered amphibolite; a typical specimen is 76-456. The rock is composed dominantly of garnet, amphibole, epidote, and biotite with minor chlorite, and albite and quartz. The garnet-rich layer contains about 70% anhedral to subhedral garnet grains with interstitial amphibole.

The texture is granoblastic.

The amphibole has the optical characteristics of actinolitic hornblende, and occurs in laths surrounding garnet grains, appearing interstitial to garnet. Hornblende laths sometimes include quartz, and are altered to a greener amphibole with a lower extinction angle and slightly higher birefringence, probably actinolite or ferroactinolite.

Epidote has anomalous interference colours and occupies a similar textural position to hornblende. The biotite is a light coloured variety with pleochroism from pale yellow to green. The biotite flakes are commonly kinked and altered, with low birefringence margins. Chlorite occurs in zones and has anomalous blue interference colours. It is a secondary mineral replacing biotite and hornblende. Plagioclase (probably oligoclase) is a minor constituent of the rock and quartz is interstitial to densely packed garnet grains and forms rare inclusions in amphibole and epidote.

The amphibole-rich layer contains larger (up to 2 mm) laths of amphibole with an interlocking texture, although they do show a crude alignment. The boundary between the layers is sharp. The garnet grains are 0.2-1.0 mm in diameter and subhedral in form. Epidote grains are anhedral, and larger than in the garnet-rich layer. Plagioclase is much more abundant, has diffuse self boundaries, and appears interstitially between the other phases. Biotite is common and is usually partly altered to chlorite with anomalous blue interference colours.

Sandblow Bay [DN038104]

A typical specimen of the body (76-479) shows that the rock is composed dominantly of amphibole, with very strong colour zoning from pale yellow to blue-green, and epidote, sphene, garnet, and oligoclase. Chlorite, biotite, quartz, and opaque minerals are present as minor constituents. The rock has a texture which tends towards lepidoblastic, but an apparently remnant texture of partially interlocking amphibole grains is present.

The amphibole is extremely variable in its optical properties, ranging from a pale coloured slightly pleochroic amphibole, probably a low iron hornblende, to a dark green to light green strongly pleochroic amphibole, probably a ferroactinolite. The ferroactinolite occurs as alteration rims to the other amphibole and as individual grains, and is probably all a secondary amphibole. The grain size ranges up to 1.5 mm. Garnet occurs in subhedral grains ranging up to one millimetre in size. Amphibole laths are deformed around the garnet grains, which have inclusions of colour-zoned amphibole, albite, and epidote.

Epidote occupies the same textural positions as amphibole and occurs with normal and anomalous interference colours in contiguous elongate grains. Plagioclase (oligoclase) is common and occurs both interstitially to other components and as an inclusion-free granular component crystallizing late in the crystallization sequence. Chlorite is an alteration product in fractures in garnet and probably biotite. The rock is cut by thin quartz veins at right angles to the alignment direction of amphibole grains. Sphene is a subhedral phase associated with ilmenite and occurs in small crystal (0.01 mm) clusters idioblastic against amphibole and epidote. It is a fairly abundant phase.

North of Trumpeter Islets [DN040078]

The garnet amphibole epidote quartz albite biotite schist is typified by specimen 76-487. The texture of this rock is porphyroblastic, with

strongly aligned amphibole laths deformed around garnet porphyroblasts. The garnet porphyroblasts constitute about 30% of the rock, are subhedral equant grains about 0.7 mm in diameter, and contain abundant quartz inclusions. They do not show an internal foliation. The amphibole is in elongate crystals and shows colourless to pale green pleochroism, sometimes with darker green, probably more iron-rich rims. It is probably an actinolite because of the low extinction angle (14°). The amphibole constitutes about 40% of the rock.

The plagioclase is untwinned (probably albite) and is xenoblastic. Biotite is relatively abundant and is aligned parallel to the schistosity. The quartz in this body is more abundant than in the other bodies, and forms clear xenoblastic grains with relatively sharp extinction. Self boundaries are diffuse and tend to form triple junctions. There is often a dimensional alignment parallel to the foliation. Epidote is common and occurs with both normal birefringence colours and anomalous colours. It is associated spatially with both biotite and ilmenite. Sphene is a common accessory mineral. Chlorite with anomalous interference colours and as an alteration product of garnet and amphibole is also present.

Davey Head [DN090044]

Typical specimens of this body are 76-493 and 76-494. The rock is lepidoblastic and is composed of amphibole, garnet, biotite, quartz, clinozoisite, plagioclase, minor muscovite, and chlorite. On the criteria identified above, the amphibole is actinolite. No alteration of amphibole occurs in these specimens. The garnet is finer grained than the amphibole and does not contain substantial inclusions. The plagioclase (albite?) is abundant, sometimes showing both simple and polysynthetic twinning, xenoblastic, and contains occasional amphibole inclusions. White-mica has a mottled extinction and is slightly pleochroic. Biotite is an alteration product from amphibole. Chlorite is present, but it is typical of a prograde metamorphic chlorite, with extremely low interference colours, rather than secondary chlorite which has anomalous blue interference colours. The epidote present has very low interference colours (probably clinozoisite). Quartz is either xenoblastic or occurs in patches in which self boundaries form triple junctions.

The body is layered, and specimen 76-493 is from an epidote-rich zone. The epidote grains are subhedral (idioblastic against actinolite) and zoned from a highly birefringent centre to a lower birefringent rim (<0.015). The rims are clinozoisite, and clinozoisite is the dominant epidote mineral in the rock. Garnet is larger in grain size (1 mm) in the epidote-rich layer, and quartz inclusions are apparent in the amphibole. Quartz is a more abundant mineral, but plagioclase, muscovite, biotite, and chlorite are absent.

Davey Head [DN089047]

This body is dissimilar to the other amphibole-bearing bodies in having a lepidoblastic texture defined by the alignment of amphibole (actinolite) and zoisite in a groundmass of plagioclase and quartz (specimen 76-495). Garnet is less abundant (<10%) and occurs as inclusion-free subhedral grains about 0.5 mm in diameter. The zoisite crystals are up to 1.5 mm long and only 0.1 mm wide. Amphibole grains are elongate in the direction of the schistosity. This body is layered, with the layering defined by a marked increase in the percentage of plagioclase and quartz and a decrease in the grain size of amphibole. The plagioclase has a refractive index below quartz and is probably albite. No mica or chlorite are present in this rock.

Summary

The amphibole-bearing rocks in the Davey Quadrangle are mineralogically and texturally variable. The following assemblages are present:

(i) actinolitic hornblende (core), ferroactinolite (rim)-garnet-epidote-plagioclase-quartz-chlorite*-biotite-ilmenite.

(ii) actinolite (zoned)-garnet-epidote-biotite-plagioclase-sphene-quartz-chlorite*-ilmenite.

(iii) actinolite-garnet-biotite*-quartz-clinozoisite-albite-muscovite-opaque minerals.

(iv) actinolite-garnet-epidote (core); clinozoisite (rim)-quartz-chlorite.

(v) actinolite-garnet-zoisite-albite-quartz.

* indicates secondary (retrograde) minerals.

The texture of the rocks ranges from granoblastic to lepidoblastic and porphyroblastic. Interlocking amphibole crystals within partly developed lepidoblastic textures are taken to indicate remnant igneous textures. The presence of abundant plagioclase in some samples indicates that the rocks are probably orthoamphibolites. The paragenesis of the rocks is discussed in more detail elsewhere.

PHYLLITE AND QUARTZ BIOTITE WHITE-MICA ALBITE SCHIST (Pp and Psb)

Phyllite occurs as thin units interbedded with quartzite or schist, and only crops out extensively on the shoreline of Kelly Basin. Most lowland areas are probably underlain by quartz schist and garnet mica schist, and no evidence for the existence of extensive areas of phyllite is present. In hand specimen, phyllite is usually a fine-grained black rock with a well developed penetrative fabric, although some green phyllite is present at Spain Bay. A silvery sheen on the foliation surface is often crinkled, producing a linear fabric. Some phyllite has porphyroblastic garnet, usually less than 3 mm in diameter. Quartz veining and the presence of widely spaced lithological banding is common in phyllite units, and complex folding is always present, varying in style from isoclinal to open.

Western shore of Bond Bay

Phyllite from this area contains small porphyroblasts of garnet and albite. A typical specimen is 77-196; this contains about 60% mica which is dominantly muscovite, but with appreciable biotite. Quartz is interlayered with micaceous bands, and albite porphyroblasts are present. The muscovite occurs in optically continuous aggregates of elongate flakes. Individual grains are well-crystallised, ranging up to 0.8 mm long. The muscovite-rich layers are deformed about albite porphyroblasts, which contain an internal foliation defined by lines of quartz grains. This internal foliation is curved and markedly discordant with the external foliation. Thus the muscovite crystallised after the albite. Biotite shows the same textural relationships as muscovite and apparently crystallised at the same time. Quartz occurs in layers and as inclusions in albite. In the quartz-rich layers the quartz is xenoblastic and has diffuse self boundaries and undulose extinction. A foliation, defined by the alignment of mica flakes, is preserved in the quartz layers; it is at an angle

to the layering and the dominant surface in the muscovite layers.

Albite is present as oval-shaped porphyroblasts about 1.5 mm long. These contain sigmoidal, discordant inclusion trails of muscovite, quartz, and biotite. All the albite tends to be porphyroblastic. Opaque minerals are common as an accessory phase.

Specimen 77-197 is of the quartz biotite white-mica albite schist body [DN096094] from this area, and is far more mica rich (>80%) and finer grained. It also has garnet porphyroblasts and only rare albite. The dominant layering, defined by thin quartz-rich layers (with an earlier foliation remnant), is clearly a crenulation cleavage, as remnant foliations are present in quartzite augen structures. Substantial zonal concentration of opaque minerals parallel to the main cleavage occurs. Chlorite is a major constituent of this rock and is present as porphyroblasts with abundant opaque minerals. It is probably the product of alteration of garnet porphyroblasts. Biotite grains are abundant and have also retrograded to chlorite. The chlorite is light green and has anomalous blue interference colours.

The garnet is partially altered to chlorite and has excellent pressure shadows formed around it. The chlorite is again associated with opaque minerals. These relationships show that both garnet, biotite, and albite grew prior to the main lithological layering in the rock, which is deformed around the porphyroblasts. Chlorite and opaque minerals grew later.

Kelly Basin

The phyllite on the western shore of Kelly Basin is a black rock, sometimes containing garnet porphyroblasts. An excellent crenulation cleavage is present in hand specimen, and is also apparent as the dominant structure in thin section. Specimens 76-467, 76-468, and 76-470 are typical examples. The dominant surface is a crenulation cleavage which has opaque minerals concentrated along the crenulation axial surfaces. The rock is very fine grained (0.05 mm), with completely anhedral feldspar (albite) grains apparently overgrowing the crenulation fabric. Slightly curved inclusion trails are totally concordant. The deformation event causing the crenulation cleavage pre-dated albite growth. The mica in this section is pale green and pleochroic, and is probably phengitic. No garnet, biotite, or chlorite are present. There is little indication as to the age of the crenulated surface.

The garnet-bearing material (76-470) is coarser grained (0.1 mm), with quartz aggregates and garnet porphyroblasts up to 2 mm. Quartz constitutes up to 60% of the rock. The dominant layering is a crenulation cleavage, as microfolds are preserved in micaceous layers. Garnet contains strongly discordant, slightly sigmoidal intrusion trails, and the external foliation is deformed around them. The rock is very similar to garnet-phyllite from Bond Bay, except that albite is absent. The number of quartz inclusions in garnets is also greater.

Spain Bay area

The phyllite at Spain Bay [DM160975] is interlayered with quartzite and quartz schist and does not form major units. It is green, rather than black, and much more homogeneous and finer grained (less than 0.05 mm) than the phyllite at Kelly Basin. The phyllite is composed dominantly of quartz (55%) and mica (40%), with small albite grains making up less than 5% of the rock. The mica is very pale green in colour and slightly pleochroic, and is

thus probably a low-iron phengite. Opaque minerals are concentrated in the axial surfaces of the crenulation cleavage, which is the dominant structural element in this area. The albite does not have inclusion trails. Typical specimens of this phyllite are 76-514 and 76-516. Chlorite is present in 76-514.

QUARTZ WHITE-MICA BIOTITE GARNET SCHIST (Psg)

This rock type is the dominant schist type in the Davey Head [DN084044] and Toogee Hill [DN046090] areas, and the rock types are excellently exposed on the west coast and along the shore of Payne Bay. The schist is coarse-grained, with garnet porphyroblasts up to 30 mm in diameter and albite laths up to 25 mm long. Mica flakes are clearly visible as crystals up to 10 mm long. Quartz rodding and veining are common, and albite tends to form in bands in the rocks. Cleavage wraps around the quartz veins, which appear to form early in the deformation sequence. The garnet occurs as dodecahedral crystals in distinct bands which parallel larger scale lithological layering. Apparent graded layering is due to the difference in the size and relative abundance of garnet porphyroblasts. Albite-rich beds show similar metamorphic layering features. Albite laths are rhomboid shaped, due to the presence of cleavages parallel to each rhomboid direction. Cleavage parallel to the dominant lithological layering is deformed around the large garnet porphyroblasts, but this warping of the foliation is not visible, in hand specimen, around albite laths.

Although garnet, biotite, muscovite, and quartz are the dominant components of most schist, plagioclase is also very abundant and thin sections show that a large variety of mineral assemblages occur within the schist areas. Quartz is present in all rock types, as are accessory or constituent opaque minerals. The mineral assemblages are shown in Figure 2.

Type	Quartz + opaque minerals	Chlorite	Garnet	Biotite	Muscovite	Plagioclase	Zoisite
1	▒	▒	▒	▒	▒		▒
2	▒	▒	▒	▒	▒	▒	
3	▒	▒	▒	▒	▒		
4	▒	▒	▒	▒			
5	▒	▒	▒		▒	▒	
6	▒	▒	▒		▒		
7	▒	▒	▒			▒	
8	▒	▒		▒			
9	▒		▒	▒	▒	▒	

Figure 2. *Mineral assemblages, quartz white-mica biotite garnet schist.*

Type 1. Specimen 76-443, Sandblow Bay [DN050100]

This rock is porphyroblastic, with 1.5 mm diameter subhedral to euhedral garnet crystals in a quartz, muscovite, chlorite matrix. There is a well defined foliation which is deflected around the garnet. The garnet contains abundant quartz inclusions, but does not always form crystals and occasionally nucleates around pre-existing quartz grains which themselves form lozenges within the dominant foliation. The grain size of quartz is the same as in the layers parallel to the foliation, which suggests that the quartz did not recrystallise during or after the deformation event which produced the foliation, as the garnet clearly grew prior to the foliation. This textural relationship implies that garnet did not grow from a distinct nucleation site, but grew as veins and stringers in the pre-existing fabric (see de Wit, 1976).

Chlorite is light green and pleochroic, showing normal low interference colours. Some flakes have pleochroic haloes, which indicates that the chlorite is secondary after biotite; this secondary chlorite is metamorphic in origin. Chlorite flakes occur parallel to the foliation and rim garnet porphyroblasts, and are also present in the matrix. Biotite is rare, but is present as thin stringers within chlorite laths. Opaque minerals are usually associated with chlorite, suggesting the breakdown reaction from biotite produced both minerals, and hence that both are secondary. The opaque minerals are xenoblastic.

Quartz has a mortar texture, with a very even grain size, straight self boundaries, and ubiquitous triple junctions. It has xenoblastic boundaries against chlorite and muscovite, while garnet forms veins around the quartz boundaries. Muscovite forms well crystallised flakes within the foliation and is biaxial negative. Muscovite also occurs as short, altered crystals in lozenges. The muscovite in these lozenges is uniaxial (?3T variety). This indicates that muscovite formed in two metamorphic events.

Zoisite is present dominantly in these lozenges, but also occurs as occasional discrete grains in the matrix. It is a length slow variety with normal low interference colours, and hence a ferrian variety. The rock contains accessory apatite. It is concluded that two metamorphic events occurred, producing garnet, zoisite, muscovite (3T), and biotite during the first event, and muscovite (probably 2M1) and chlorite in the second event. The crystallisation of chlorite and opaque minerals was at the expense of biotite.

Type 2. Typical specimens 76-451, 76-463, 76-486, 76-488, 76-499.

This schist type is volumetrically the most abundant type in the quadrangle, and is best exposed along the west coast from Sandblow Bay to north of Trumpeter Islets [DN039077]. Specimen 76-451 [DN039105] contains abundant plagioclase clasts up to 5 mm long, with abundant quartz and muscovite inclusions. These inclusions form discordant, slightly sigmoidal inclusion trails, indicating that the plagioclase is an early mineral. The plagioclase shows multiple twinning and is optically positive. The relief is lower than quartz (Becke line test). It is thus albite. Biotite and muscovite are abundant, and chlorite occurs in sheaths of the other sheet silicates which surround the albite laths. Chlorite, biotite, and opaque minerals are intimately associated, and chlorite also appears secondary after garnet. Garnet is present as rounded grains or euhedral crystals in albite laths and overgrowing quartz/mica grain boundaries. No deformation occurs around the grains, and the garnet appears mimetic. Rare grains of a clear, high relief mineral with very low birefringence occur (probably

zoisite); this grew at the same time as garnet.

Specimen 76-453 [DN038089] shows different textural relationships. The albite laths are untwinned but have concordant inclusion trails, and the garnet is better crystallised with no or only very few inclusions. The deflection of the foliation around the garnet grains is minor; no pressure shadows have formed and garnet alteration is minor. Garnet grew very late in the deformation event producing the foliation. Chlorite is again abundant, and has normal interference colours. Chlorite with anomalous colours occurs close to skeletal garnet, as well as in cracks in garnet porphyroblasts. Biotite is abundant and occurs in the centre of garnet rims. Consequently, in this section, the garnet is interpreted as late with respect to the foliation formation, and the albite is interpreted as forming during deformation. Chlorite is again probably after earlier biotite, and anomalous chlorite is later than the main tectonic surface.

Specimen 76-454, from the same locality, shows very similar features, except that subhedral garnet grains with discordant inclusion trails cause deflection of the foliation. Numerous garnet grains have a central region with abundant inclusions of quartz, rimmed with clean garnet. Garnet grains with no inclusions and clear skeletal garnet show no deflection of the foliation. These features suggest that there are two phases of garnet growth, one associated with an earlier tectonic surface, and the other late in the later, main foliation forming event. Albite in this specimen has recrystallised syntectonically with the main foliation forming event.

Abundant, small poikiloblastic garnets (<0.1 mm) which are post-tectonic occur in specimens 76-461 [DN038092] and 76-486 [DN039078]. In these specimens, porphyroblastic albite deflects the foliation and has discordant inclusion trails. Thus the earlier event produced only albite and biotite. In specimen 76-463 [DN039093], rimmed garnet and poikiloblastic garnet are present. The albite porphyroblasts are earlier than the foliation. In specimen 76-488, a much higher percentage of biotite is present (up to 30%) and this is partially altered to chlorite. Garnet is a minor component and occurs as small skeletal or poikiloblastic grains. Specimen 76-499 contains both clear and rimmed garnets. The small, clear garnet is evenly dispersed, crystallises across grain boundaries, and is a late phase.

From these textures, it is clear that two major metamorphic events occurred throughout the area, and that the development of mineral phases within each event was controlled by a process of metamorphic layering, visible in the field. Both metamorphic events reach P-T conditions in some layers suitable for the development of garnet schist, and in some cases epidote schist. However, not all layers formed these minerals in each event.

Type 3. South shore of Kelly Basin [DN098069]

This rock type differs from Type 2 schist in that no plagioclase is present, and the biotite is well crystallised and not altered to chlorite. The chlorite is pale green and has normal, low interference colours. It has sharp boundaries with biotite and muscovite, and hence may represent an equilibrium metamorphic assemblage. Garnet occurs in subhedral to euhedral porphyroblasts, with partial warping of the foliation and good development of pressure shadows of quartz behind porphyroblasts. These factors imply that the foliation formed after the porphyroblasts.

Type 4. West coast, north of Gulches Reef [DN039093]. Typical specimens 76-464, 76-465, 76-472

Absence of muscovite characterises this rock type, which is very garnet-rich (25%). Quartz constitutes about 60% of the rock, and the remainder is composed of equal amounts of biotite and chlorite with minor opaque minerals, plagioclase, and zoisite. In specimen 76-464 [DN039093] there are two varieties of garnet. The first forms porphyroblasts, with very few inclusions, an even grain size (≈0.4 mm) and a rounded to euhedral form; and the second forms larger porphyroblasts (8-10 mm) with euhedral (square) interior zones poikilitically enclosing quartz and surrounded by a substantial rim of clean garnet with fewer fractures, similar to the small porphyroblasts. Clearly there were two phases of garnet growth. Zoisite is an abundant mineral phase in this specimen, is euhedral in form, and contains quartz and muscovite inclusions. Biotite is parallel to early cleavage surfaces preserved as microfolds between the dominant crenulation cleavage zones, and hence was formed during the early metamorphic event. In the later event, chlorite with normal interference colours formed parallel to the dominant crenulation cleavage, probably replacing biotite. The plagioclase is albite (+ve, low relief), and is only a minor constituent of the rock. It is usually untwinned, and forms in textural continuity with the groundmass of the rock in quartz-chlorite-biotite stringers. It is deflected around garnet with the foliation and is thus formed synchronously with the main cleavage. It contains numerous inclusions.

Specimen 76-465 [DN039093] is similar to this, except that garnet is more abundant and chlorite is present in two forms, one with normal interference colours and one with anomalous colours. The latter is later than the former, and is a product of breakdown of biotite, chlorite with normal colours, and garnet. Quartz occurs in isolated equigranular patches with mortar texture. The patches are remnants of an earlier lithological layering. In specimen 76-472, garnet porphyroblasts are associated with pressure shadows and appear to have developed early in, or prior to the development of the cleavage. The garnet is clear and does not contain overgrowth rims. Neither specimen 76-465 nor 76-472 contains plagioclase or zoisite.

The textural evidence from these specimens implies that garnet growth occurred prior to the main crenulation cleavage, and later smaller porphyroblasts nucleated during a second deformation event and continued growth and new nucleation until after that event ended. Zoisite occurs sporadically, in patches, and formed during the first metamorphic event.

Type 5. West coast [DN039098]. Specimen 76-474

This rock is characterised by the development of rims around garnet porphyroblasts. Euhedral garnet is surrounded by rims of fine-grained quartz, and this is succeeded by a rim of garnet. Inclusions in the euhedral core are not aligned and not abundant. Alteration of garnet to anomalous chlorite is common. Garnet without an interior zone overgrows muscovite-quartz boundaries, and does not cause foliation deflection. Quartz rims formed during the second cleavage prior to the nucleation of new garnet, also implying that garnet is a late phase in this rock. Plagioclase (albite) is slightly porphyroblastic, but contains concordant inclusion trails. It crystallised during the development of the main cleavage. Chlorite has anomalous blue interference colours and is associated with minor biotite and opaque minerals. It is a post-tectonic retrograde metamorphic mineral. Muscovite is euhedral in large flakes and is synchronous with the main

cleavage. It is deformed by later folds.

Type 6. West coast. Typical specimens 76-485, 76-462.

This schist type is the second most abundant variety, and is characterised by the absence of albite porphyroblasts and only rare biotite grains. Garnets are commonly large (up to 15 mm) and nearly always contain rim overgrowths (*e.g.* 76-462). The core usually contains quartz poikilitically, and is occasionally surrounded by a thin rim of quartz. The annular rim garnet is much clearer of inclusions. Muscovite is very coarse grained (4-5 mm). Biotite does occur, but is usually altered to chlorite in these rocks. Alteration of garnet is also common. In specimen 76-476, anomalous chlorite occurs in garnet pressure shadows, and no indication of its origin remains. Biotite is absent. In specimen 76-484 there is an indication that the rims of garnet contain straight, discordant inclusion trails, and the foliation is deflected around both rims and cores of the very large garnet porphyroblasts. Specimen 76-485 is similar, but contains chlorite with normal interference colours as well as chlorite with anomalous colours. Zircon included within the normal coloured chlorite produced pleochroic haloes, which affects both types of chlorite. They are both therefore derived from biotite, and the blue chlorite is later than the normal chlorite. A yellowish colour in normal light suggests that the anomalous chlorite is more iron-rich.

Type 7. Opposite Gulches Reef [DN038078]. Specimen 76-457.

This rock contains both garnet and albite porphyroblasts, but is free of muscovite. Retrograde metamorphic effects are emphasised in this rock, chlorite being the most abundant mineral, with both anomalous and normal types. Twinned albite partly surrounds garnet porphyroblasts which both crystallised together. Quartz is very fine grained and constitutes less than 10% of the rock. Some altered matrix plagioclase is present. Chlorite constitutes up to 80% of the rock. The rock type is volumetrically minor in the sequence.

Type 8. Opposite Gulches Reef [DN038078]. Specimen 76-460.

This is also a volumetrically minor rock type, and contains no garnet or plagioclase. It is a fine-grained schist (<0.1 mm) and has quartz-rich and biotite-rich layers. The quartz constitutes about 30% of the rock, the remainder being composed of stubby biotite, normal chlorite, and minor anomalous chlorite grains forming an interlocking framework. Chlorite is dominant over biotite.

Type 9. Davey Head [DN080047]. Specimen 76-496.

Albite, with abundant quartz inclusions and large biotite flakes characterise this type, but no garnet is present. Quartz is fine-grained and poikilitic throughout the section (<0.02 mm), and well crystallised muscovite is fairly abundant along albite grain boundaries. Albite is usually untwinned, and opaque minerals are common. No chlorite is present. A weak foliation is defined by biotite alignment.

The extreme variation in mineralogy and texture of schist types shows that conditions of metamorphism and probably original composition varied over the area. The rocks are generally metamorphosed to the garnet zone of the greenschist facies, but examples of non-garnetiferous schist and schist with no plagioclase or chlorite indicate that conditions were complex. Two major metamorphic episodes occurred, but the variation in time of development of the second event, with respect to deformation

processes, produced a variety of textures and mineralogies within the metamorphic body. Metamorphic layering appears to have developed in both the major metamorphic episodes.

QUARTZ WHITE-MICA SCHIST (Pqs) AND QUARTZITE (Pq)

The dominant rock type in the Davey Quadrangle is quartzite, with some areas of quartz schist and quartz-mica schist occurring in valleys and on hill sides. The areas around Coffin Bay [DN165085] and Spain Bay [DM165975] are composed almost exclusively of these two rock types. In hand specimen, the quartzite is white and hard, with individual quartz grains visible. Outcrops are flaggy, with a cleavage-parallel parting spaced at 20 mm to 200 mm. The parting planes are parallel to joints and do not always represent a lithological layering. The quartzite sequence at Berry Head [DN150073] is layered, with thin bands of green quartzose phyllite separating quartzite layers up to 220 mm thick. Apparent cross-bedding is a common feature of the quartzite, but this is not a true sedimentary structure (see section on meso-structures). Mesoscopic folding, both open and isoclinal, is a common feature of the quartzite units.

Quartz white-mica schist is a more micaceous rock type, with the rock parting into layers less than 50 mm thick. The amount of white mica in the rocks is variable, but it is abundant on and aligned parallel to the parting surfaces. The rock type grades into quartzite with a reduction in mica content, and also into quartzose phyllite with a reduction in grain size and increase in mica content. Some fine-grained layers in units mapped as quartz white-mica schist are mica poor, and resemble metasiltstone (*e.g.* Wallaby Bay, DN158068). At Hilliard Head [DM130960] the area mapped as quartz white-mica schist consists of quartz-schist finely interlayered with micaceous quartzite. Quartzose phyllite, quartz white-mica schist, and thin quartzite units are interlayered at Mutton Bird Island [DM163920], with the more micaceous units predominating. Consequently areas mapped as Pqs are more heterogeneous and mica-rich domains, whereas areas mapped as Pq are strongly dominated by massive to flaggy quartzite with a grain size gradation from 0.2 mm to 2.0 mm.

Quartzite units in the Davey Head area are typified by specimens 76-480 and 76-481. The percentage of muscovite present is very low (<1%), and concentration of muscovite shows a crude lithological banding across which quartzite grain size changes occur. The scale of this banding is in the order of one millimetre thick. A weak dimensional preferred orientation of quartz grains is present but has been partially annealed, giving the rock a tendency to be granoblastic. A good mica alignment is parallel to the dimensional quartz fabric. Quartz grain boundaries are sutured and triple junctions are common. Mica flakes average 0.1 mm long and quartz grains are up to 0.2 mm in size. Opaque minerals are an accessory component of the rock.

Pure quartzite crops out on the plains between Kelly Basin and Saddle Bight (specimen 76-497, DN098060). The grain size is up to 1.5 mm and the grains show a good dimensional preferred orientation. Grain boundaries are strongly sutured and stylolitic. Deformation lamellae are continuous in orientation across all grains, indicating a tendency towards preferred crystallographic orientation in the grains. Intergranular areas are composed of fine-grained (<0.05 mm) granulated quartz.

North of Whalers Point [DN124060] quartz white-mica schist contains albite porphyroblasts with discordant inclusion trails. The rock has a ribbon texture, with quartz-albite lozenges separated by biotite and

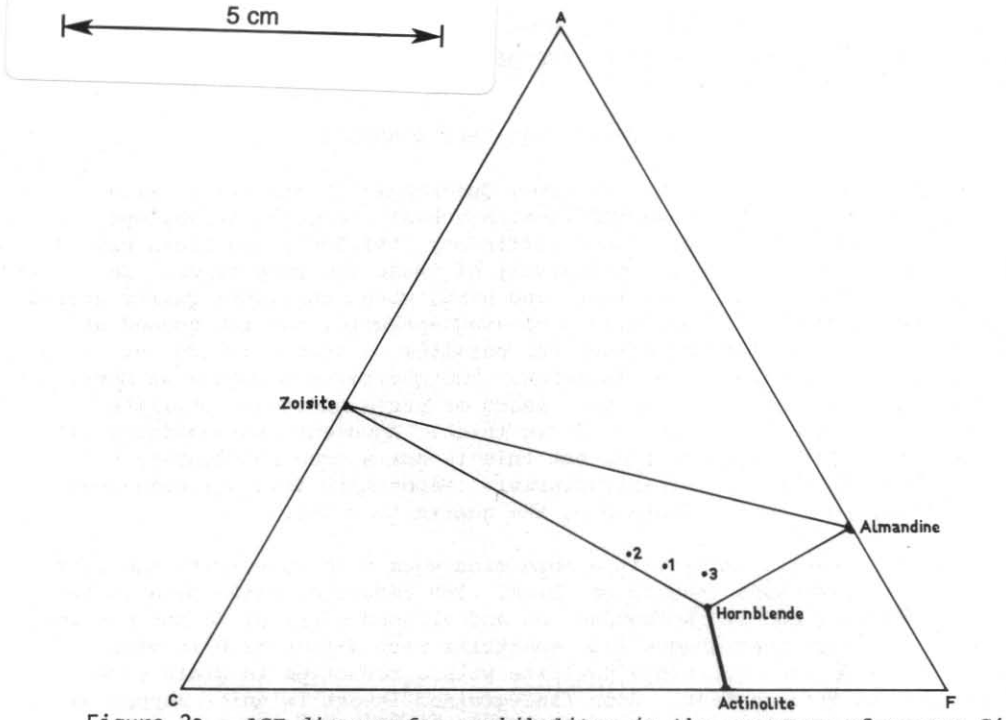

Figure 3a. *ACF diagram for amphibolites in the presence of excess SiO_2 as free quartz. A = Al_2O_3 + Fe_2O_3 - (Na_2O + K_2O); C = CaO; F = FeO + MgO + MnO. Oxides are expressed as molecular proportions. Plots indicate an amphibolite facies equilibrium assemblage.*

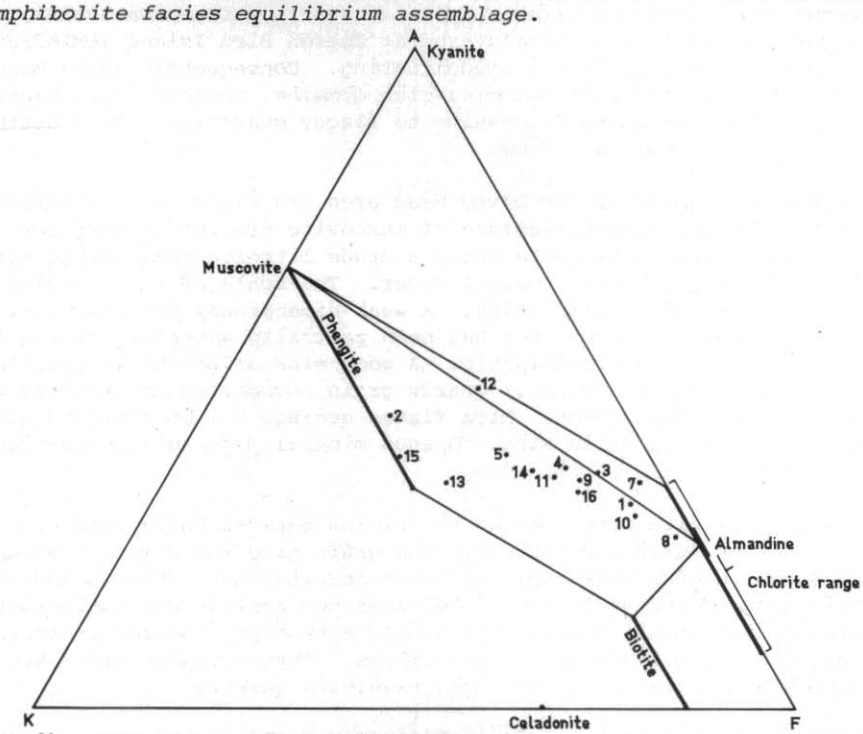

Figure 3b. *AKF diagram for pelitic schist in the presence of excess SiO_2 as free quartz. A = Al_2O_3 - (CaO + Na_2O + K_2O); K = K_2O; F = FeO + MgO + MnO. Plots are coincident with an amphibolite facies equilibrium assemblage.*

muscovite sheaths and layers. The quartz schist unit at South East Bight [DN065045] again contains abundant plagioclase (albite) grains, but they are not porphyroblastic (77-201). In thin section, abundant biotite is present as well as white-mica. Small garnet grains also occur. Deformation of the foliation suggests that albite formed prior to the dominant cleavage Mica (both biotite and muscovite) constitute between 40% and 50% of these specimens. The quartz mica schist at Hilliard Head [DM133972] is composed of up to 80% pleochroic muscovite (phengite) and also contains small albite laths with discordant inclusion trails. Quartzite in the Hannant Point area [DM170989], typified by specimen 76-515, shows far less recrystallisation, with large grains showing strain features (undulose extinction and boundary dissolution) surrounded by small, weakly aligned neocrystalline quartz grains. This is a mortar texture. Phengite comprises between 5% and 10% of the rock.

Quartzite is the most areally extensive rock type in the Coffin Creek area. Recrystallisation and later annealing are common (77-7, 77-8), and is similar to quartzite in the Davey Head area. Where muscovite is absent, there is a better developed dimensional preferred orientation of quartz, and very fine-grained opaque material is concentrated along grain boundaries (77-9). Specimen 77-10 is more micaceous [DN176067], with the micaceous material (sericitic) in seams paralleling the preferred quartz orientation.

Quartz white-mica schist (Pqs) from Wallaby Bay (77-16, DN158068) is very fine-grained (≈0.02 mm) and is composed of strongly aligned phengite grains with layers of quartz and albite grains. Opaque minerals are abundant, and tourmaline (green to very dark green pleochroism) is an accessory mineral. Altered biotite is also present.

MINERALOGY AND CHEMISTRY OF THE PRECAMBRIAN ROCKS

Chemical analyses of whole rocks and individual minerals from the schist in the Davey Quadrangle are concentrated on the coarse-grained rocks occurring around Davey Head and on the west coast opposite Trumpeter Islets. Eighteen specimens were analysed at the Department of Mines Launceston Laboratories by J. Furst using XRF techniques. The results of these analyses are shown in Table 1, and triangular diagrams are plotted from these analyses (figs. 3a, 3b). The fields of various minerals are also shown. The AKF diagram (fig. 3a) shows that there is a wide spread of iron content in the schists, but that all fall within the stability field muscovite-biotite-almandine, which is consistent with their mineralogy. Samples which lie above the almandine-muscovite join, and also numerous other samples,contain chlorite as well as garnet, a disequilibrium situation due to the formation of chlorite in a later stage of metamorphism. The rocks are not sufficiently aluminous to fall into the kyanite-muscovite-almandine field, and the absence of crossing tie-lines suggests that the early metamorphic event may have reached equilibrium.

The ACF diagram (Eskola, 1939) for three amphibolites or amphibole-epidote schists (fig. 3b) shows that the bulk composition and mineral composition of these rocks is compatible, and that the assemblages are representative of the medium grade (amphibolite facies), although some are representative of low grade (upper greenschist facies). No corrections have been made to either of these diagrams, because the modal percentage of apatite, ilmenite, and sphene is generally too low to affect the diagrams. Magnetite and calcite are absent.

Table 1. CHEMICAL ANALYSES OF SCHIST AND AMPHIBOLITE FROM THE PORT DAVEY AREA

Sample	760938 PD 1	760955 PD 3	760939 PD 9	760940 PD14	760941 PD21	760942 PD22	760943 PD23	760944 PD32	760945 PD39
SiO_2	70.60	63.10	65.80	67.30	59.40	68.60	58.00	51.80	46.30
TiO_2	0.83	0.57	0.38	0.47	0.71	0.53	0.63	1.60	1.30
Al_2O_3	11.40	15.10	17.10	12.60	17.70	15.90	13.20	14.10	15.20
Cr_2O_3	0.00	0.00	0.00	0.00	0.00	0.00	0.00	0.00	0.00
Fe_2O_3	0.91	2.40	2.90	2.60	2.30	0.98	8.50	3.60	2.70
FeO	8.00	8.30	0.66	8.20	8.80	4.50	9.60	16.60	11.20
MnO	0.09	0.12	0.02	0.27	0.30	0.07	0.60	0.22	0.25
MgO	3.30	2.20	2.10	2.30	2.50	1.50	5.00	6.20	7.80
CaO	0.23	0.26	0.07	0.62	0.37	0.20	1.00	0.26	9.80
Na_2O	0.14	1.20	0.15	0.18	0.50	1.60	0.40	0.04	2.00
K_2O	1.60	3.50	7.10	2.40	4.00	4.00	1.10	1.20	1.10
P_2O_5	0.13	0.07	0.04	0.11	0.03	0.06	0.08	0.11	0.10
H_2O^+	2.90	3.40	2.90	2.10	2.80	2.10	2.60	3.80	2.80
H_2O^-	0.03	0.10	0.07	0.00	0.00	0.00	0.00	0.00	0.00
L.O.I.	0.00	0.00	0.00	0.00	0.00	0.00	0.00	0.00	0.00
CO_2	0.13	0.08	0.10	0.17	0.34	0.22	0.21	0.27	0.27
Total	100.29	100.40	99.39	99. 32	99.75	100.26	100.92	99.80	100.82
AMG ref.	DN05061011	DN04301069	DN03101055	DN03730891	DN03790922	DN03790922	DN03790922	DN03930975	DN03801042
Rock type	Garnet schist	Albite schist	Mica schist	Garnet schist	Garnet schist	Albite schist	Garnet schist	Garnet schist	Amphibolite

Analyst: J. Furst, Department of Mines, Launceston.

Table 1. (continued)

Sample	760946 PD44	760947 PD45	760948 PD46	760949 DH 1	760950 DH 2	760951 DH 9	760952 DH15	760953 DH16	760954 SB 3
SiO_2	63.60	55.10	65.70	48.20	47.70	60.00	70.80	68.50	64.80
TiO_2	0.60	0.51	0.60	1.10	0.83	0.88	0.44	0.64	0.39
Al_2O_3	15.70	16.90	15.80	15.00	16.10	20.70	15.10	15.30	18.10
Cr_2O_3	0.00	0.00	0.00	0.00	0.00	0.00	0.00	0.00	0.00
Fe_2O_3	1.50	1.50	1.50	3.40	1.80	1.00	0.52	0.83	2.10
FeO	8.50	13.90	6.50	8.40	9.30	4.40	2.70	4.30	0.92
MnO	0.14	0.38	0.39	0.22	0.26	0.08	0.05	0.13	0.07
MgO	2.60	4.10	1.40	8.30	10.40	1.40	1.30	1.40	2.30
CaO	0.29	0.48	0.56	11.50	8.10	0.42	0.26	0.65	0.03
Na_2O	0.31	0.23	1.80	1.80	3.30	1.10	1.70	2.30	1.20
K_2O	3.40	2.50	3.30	0.08	0.12	4.50	5.10	3.10	7.40
P_2O_5	0.09	0.12	0.12	0.07	0.02	0.08	0.10	0.09	0.00
H_2O^+	3.70	3.70	2.40	2.30	2.20	4.30	2.40	2.40	3.30
H_2O^-	0.00	0.00	0.00	0.00	0.00	0.19	0.03	0.02	0.00
L.O.I.	0.00	0.00	0.00	0.00	0.00	0.00	0.00	0.00	0.00
CO_2	0.24	0.22	0.20	0.15	0.15	0.20	0.28	0.28	0.10
Total	100.67	99.64	100.27	100.52	100.28	99.25	100.78	99.94	100.71
AMG ref.	DN03930777	DN03930777	DN04020787	DN09060443	DN09000437	DN10990837	DN11950487	DN09670373	--
Rock type	Garnet schist	Garnet schist	Albite schist	Amphibolite	Amphibolite	Garnet schist	Quartz schist	Albite schist	Quartz schist

Location of each sample and a description of the rock types are contained in Appendix 1.

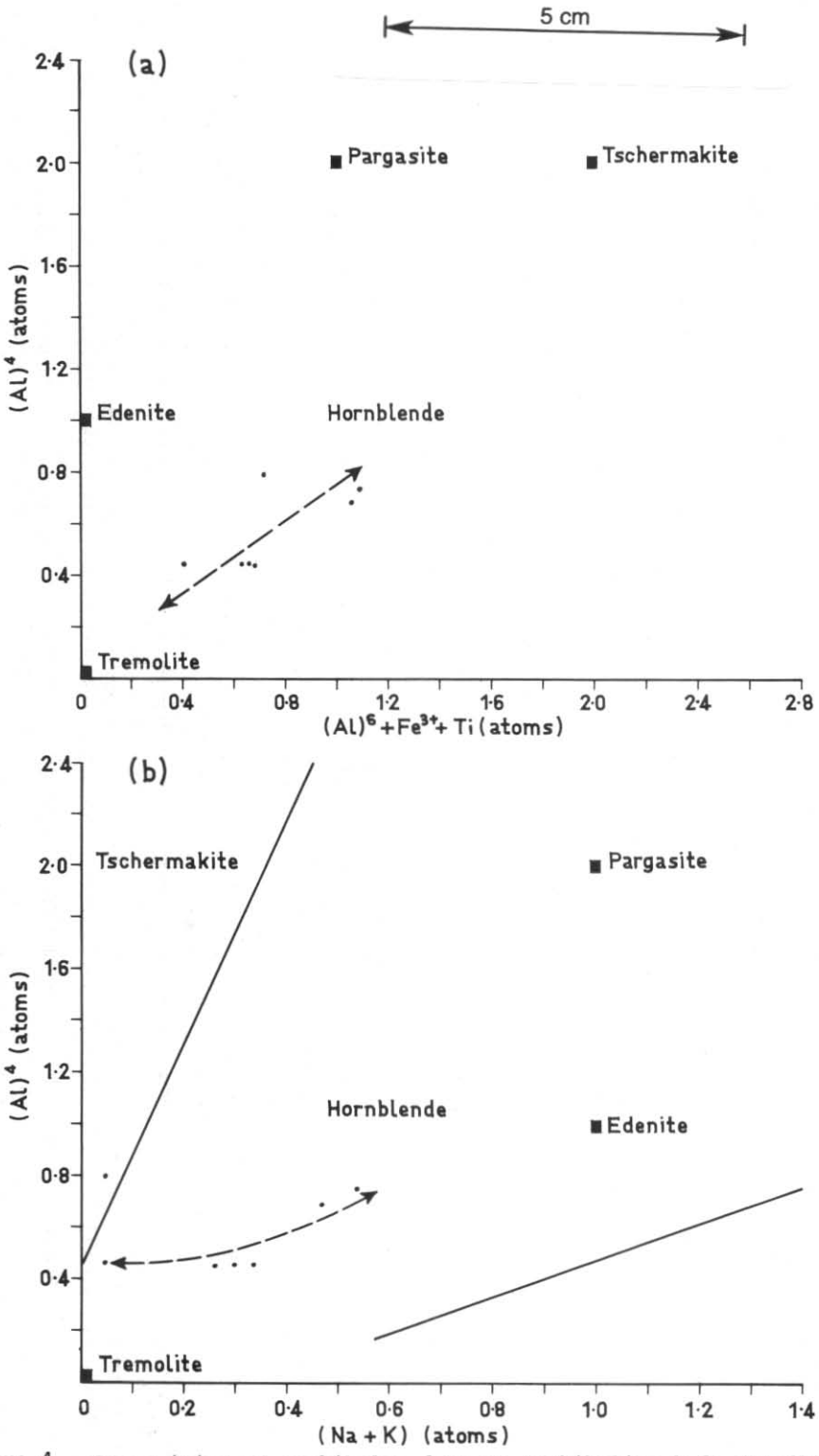

Figure 4. *Composition of amphiboles from an amphibolite body (Sandblow Bay) expressed as octahedral aluminium, ferric iron and titanium atoms (2a) and the number of Na and K atoms (2b) compared to tetrahedral aluminium in a formula unit. The diagrams show the zonation of hornblende towards a tremolite composition. In all analyses $Mg>Fe^{2+}$ and in all but one analysis $Mg>>Fe^{2+}$.*

AMPHIBOLITE AND AMPHIBOLE-EPIDOTE SCHIST

Individual mineral analyses (Table 3) were carried out at the University of Tasmania Central Science Laboratory using a Jeol JXA-50 electron probe microanalyser. The results of analysis of amphibole from the amphibolite and amphibole schist bodies are shown in Table 2. The microprobe data have been recalculated to determine the ratio of FeO to Fe_2O_3 in the amphibole using the assumptions of Papike *et al.* (1974). These are that: (i) the total cationic charge equals 46; (ii) all coupled substitutions charge balance, and (iii) no octahedral site deficiencies occur. Analyses which failed any of these criteria are not reported. The calculation assumes the maximum Fe_2O_3 value possible consistent with crystal chemical criteria. The structural formula of each amphibole is calculated using these values. All amphiboles have a substantial octahedral site excess, but only a minor component of this is present in the A site, which is occupied by potassium atoms. The minerals are aluminous calciferous amphiboles (common hornblende) which vary from the tremolite/actinolite field to the hornblende field. Petrographically, zonation of amphibole is visible, the outer rims being more actinolite-rich and the inner rims more calcic. This compositional zonation is shown in Figure 4, and may be related to retrograde metamorphism associated with the production of chlorite.

Analyses of the other components of the amphibolite confirm that zonation of minerals during metamorphism is significant. The manganese content of the garnet varies from 0.85% in the rim to 2.6% in the core, and the iron content of chlorite is similarly variable (22.7%-28.75%, disparate totals equalised to highest). Although zonation during prograde metamorphism is well documented (de Wit, 1976; Råheim, 1975), the marked zonal nature of the amphibole and the often physically distinct chlorite crystals with different birefringence and composition strongly suggests that the mineralogy has been altered by retrograde metamorphism. A medium grade (amphibolite facies) assemblage is implied by the absence of primary chlorite, the presence of garnet, the hornblende core composition, and the presence of oligoclase (An 19) (Winkler, 1979). The only representative of low grade assemblages (greenschist/amphibolite transition facies) is at Davey Head, where albite and primary chlorite are present in co-existence with garnet. The grossular content of the garnet is high, considering the almandine-rich nature of the mineral, and is substantially higher than for garnet in schist. The two analyses of sheet silicates show that the mica component is chemically complex, analysis 180 being too silica-rich for a true muscovite and analysis 182 being too silica-rich and too iron-poor for a true chlorite. These probably represent altered muscovite and altered biotite respectively. The assemblage indicates a temperature of about 500°C (Winkler, 1979) at moderate pressure.

GARNET-RICH SCHIST

Three garnet-mica schist specimens (76-443, 76-462, 76-463) have been analysed using the microprobe. The results of the analyses are presented in Table 4. Specimen 76-443 contains a moderately pyrope-rich garnet and Mg-rich chlorite. In addition to the phases analysed, zoisite grains and apatite crystals are present. The apatite is shown in Figure 5 as discrete grains rather than needle-like accessory minerals; these are probably a product of metamorphism. The white-mica is strongly phengitic (Fe^{2+} + Mg = 1.17 atoms). The absence of cordierite or staurolite in this rock suggests that temperatures were below 540°C, assuming pressures of about 400 MPa (Hoschek, 1969) and that the rock belongs to the low temperature assemblage of Winkler (1979), of relatively high pressure. The assemblage during the second metamorphic event; almandine/pyrope + chlorite + biotite + phengite +

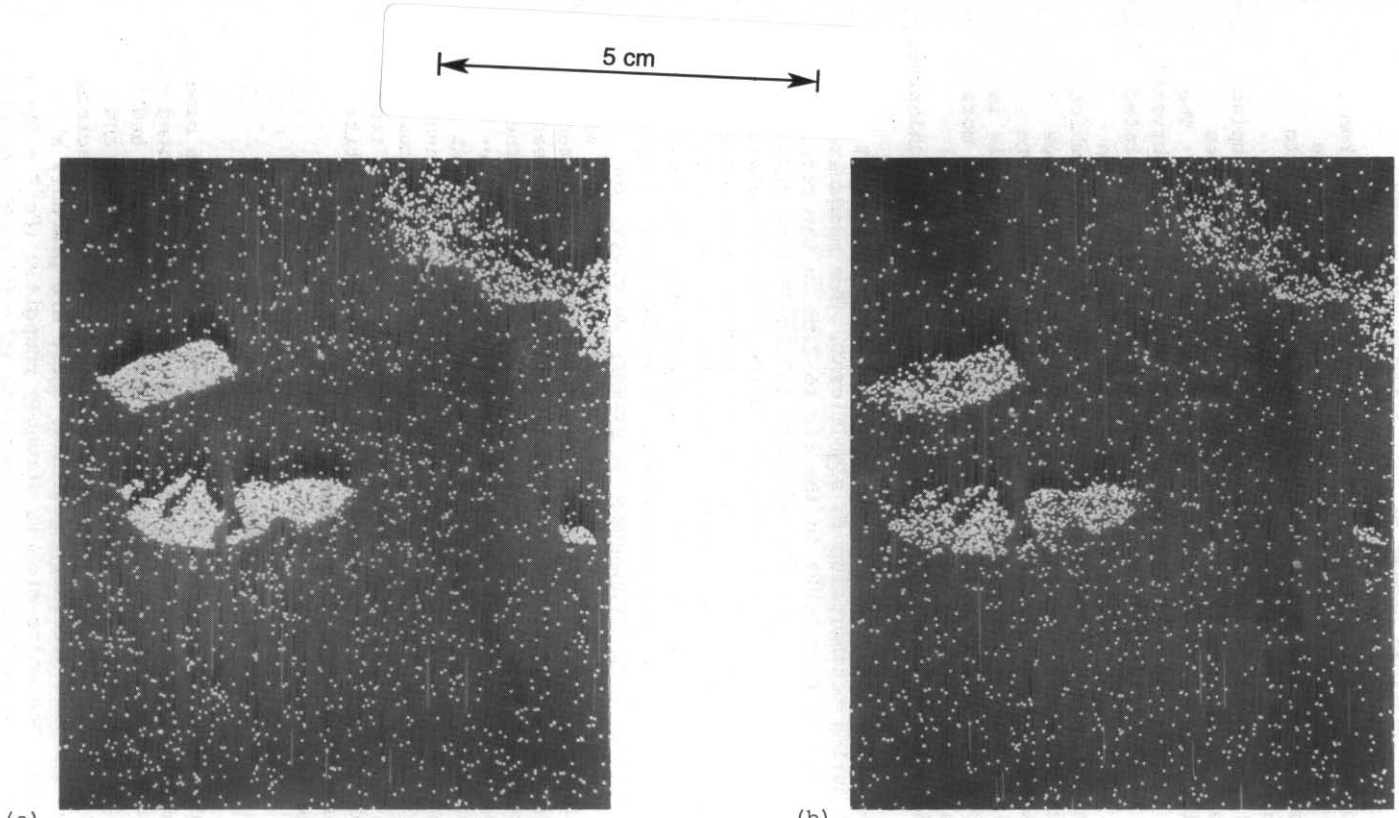

Figure 5. *X-ray maps of calcium (a) and phosphorous (b) over an area of slide 76-445, showing the presence of apatite grains. Magnification x 100.*

Table 2. CHEMICAL ANALYSES OF AMPHIBOLE GRAINS FROM AN AMPHIBOLITE FROM SANDBLOW BAY [DN038104]

SiO_2	53.16	50.31	53.39	55.19	53.24	48.11
TiO_2	0	0.13	0.15	0.15	0	0.32
Al_2O_3	5.84	8.35	5.65	6.07	4.42	7.58
Cr_2O_3	0.2	0.18	0.2	0.18	0.16	0.25
Fe_2O_3	0	0	0	0	0	0
FeO	9.46	11.72	9.10	9.12	11.31	14.22
MnO	0	0	0	0	0	0
MgO	17.05	13.86	17.21	17.58	16.35	12.37
CaO	9.99	8.97	10.05	10.44	12.58	11.73
Na_2O	0.81	1.52	0.98	1.09	0	0
K_2O	0.22	0.19	0.23	0.37	0.28	0.24
Total	99.63	95.23	96.96	100.17	98.34	94.82
Si	7.55	7.31	7.55	7.55	7.55	7.20
Al	0.45	0.69	0.45	0.45	0.45	0.80
Σ	8.00	8.00	8.00	8.00	8.00	8.00
Al	0.53	0.74	0.49	0.53	0.29	0.54
Ti	0	0.01	0.02	0.02	0	0.04
Fe^{3+}	0.11	0.32	0.16	0.11	0.11	0.14
Fe^{2+}	1.01	1.10	0.92	0.94	1.23	1.64
Mg	3.61	3.00	3.63	3.59	3.46	2.76
Σ	5.26	5.17	5.22	5.19	5.09	5.12
XM_{1-3}	0.26	0.17	0.22	0.19	0.09	0.12
Ca	1.52	1.40	1.52	1.53	1.91	1.88
Na	0.22	0.43	0.26	0.28	0	0
Σ	2.00	2.00	2.00	2.00	2.00	2.00
Na	0	0	0.01	0.01	0	0
K	0.04	0.04	0.04	0.06	0.05	0.05
Σ	0.04	0.04	0.05	0.07	0.05	0.05

Analyses obtained using Jeol JX-50A Electronprobe microanalyser at the Central Science Laboratory, University of Tasmania. The structural formulae are calculated according to assumptions given by Papike *et al.* (1974).

Table 3. CHEMICAL ANALYSES OF INDIVIDUAL MINERAL PHASES IN AN AMPHIBOLITE FROM SANDBLOW BAY [DN038104]

Mineral:	Chlorite*	Chlorite	Chlorite	Mica†	Mica	Epidote	Epidote
SiO_2	23.86	26.03	26.23	57.75	45.06	39.62	38.16
TiO_2	0	0.10	0	0.12	0.42	0	0.17
Al_2O_3	19.83	20.18	21.61	18.90	22.27	29.14	25.59
Cr_2O_3	0	0.18	0	0	0.17	0	0.16
Fe_2O_3	0	0	0	0	0	0	0
FeO	32.90	28.91	22.84	1.32	13.98	5.03	10.82
MnO	0	0.14	0	0	0	0	0
MgO	12.39	13.15	16.91	0	5.28	0	1.35
CaO	0	0	0	4.34	5.46	24.21	20.64
Na_2O	0	0	0.80	0	1.65	0	0
K_2O	0	0	0	13.12	1.40	0.08	1.22
H_2O	11.02	11.30	11.62	4.45	4.31	1.93	1.87
Total	100.00	100.00	100.00	100.00	100.00	100.00	100.00
			STRUCTURAL FORMULAE				
No. Oxygen	28	28	28	22	22	25	25
Si	5.19	5.52	5.41	7.78	6.26	6.15	6.12
Al	2.81	2.48	2.59	0.22	1.74	0	0
Σ	8.00	8.00	8.00	8.00	8.00	6.15	6.12
Al	2.27	2.57	2.66	2.79	1.92	5.34	4.83
Ti	0	0.02	0	0.01	0.04	0	0.02
Cr	0	0.03	0	0	0.02	0	0.02
Fe^{3+}	0	0	0	0	0	0	0
Fe^{2+}	5.98	5.13	3.94	0.15	1.63	0.65	1.45
Mn	0	0.03	0	0	0	0	0
Mg	4.02	4.16	5.20	0	1.09	0	0.32
Σ	12.27	11.93	11.80	2.95	4.70	-	-
Ca	0	0	0	0.63	0.81	4.03	3.54
Na	0	0	0.32	0	0.45	0	0
K	0	0	0	2.26	0.25	0.02	0.25
Σ	0	0	0.32	2.89	1.51	-	-
OH	16.00	16.00	16.00	4.00	4.00	2.00	2.00

Analyses obtained using a Jeol JX-50A Electronprobe microanalyser at the Central Science Laboratory, University of Tasmania. Analyses have been recalculated assuming all iron is in the bivalent state and the minerals contain ideal water.

All analyses from specimen 76-479.

* Analysis 182
† Analysis 180

Table 3 (continued).

Mineral:	Sphene	Ilmenite	Plagioclase*	Garnet† (1)	Garnet† (2)	Garnet† (3)
SiO_2	30.14	0.32	63.14	36.70	37.83	37.32
TiO_2	40.33	52.28	0	0.36	0.23	0.35
Al_2O_3	0.87	0	23.11	20.84	21.75	21.33
Cr_2O_3	0.22	0.22	0.12	0.24	0.25	0.20
Fe_2O_3	0	0	0	0	0	0
FeO	0	43.20	0.14	25.94	25.75	25.78
MnO	0	3.56	0	2.11	0.85	2.61
MgO	0	0	0	2.91	3.48	3.18
CaO	28.43	0.42	3.95	10.54	9.87	9.16
Na_2O	0	0	9.45	0	0	0
K_2O	0	0	0.10	0.36	0	0.07
H_2O	0	0	0	3.51	0	0
Total	100.00	100.00	100.00	100.00	100.00	100.00
			STRUCTURAL FORMULAE			
No. Oxygen	20	6	32	12	12	12
Si	3.93	0.02	11.17	2.93	2.97	2.96
Al	0	0	-	0.07	0.03	0.04
Σ	3.93	-	-	3.00	3.00	3.00
Al	0.14	0	4.82	1.89	1.98	1.95
Ti	3.96	1.98	0	0.02	0.01	0.02
Cr	0.02	0.01	0.02	0.02	0.02	0.01
Fe^{3+}	0	0	0	0	0	0
Fe^{2+}	0	1.82	0.02	1.73	1.69	1.71
Mn	0	0.15	0	0.14	0.06	0.18
Mg	0	0	0	0.35	0.41	0.38
Σ	-	-	-	-	-	-
Ca	3.98	0.02	0.75	0.90	0.83	0.78
Na	0	0	3.24	0	0	0
K	0	0	0.02	0.04	0	0.01
Σ	-	-	-	-	-	-
OH	0	0	0	0	0	0

Plagioclase*

(mol %)	
Orthoclase	0.52
Albite	80.18
Anorthite	19.30

Garnet†

(mol %)	(1)	(2)	(3)
Pyrope	9.61	11.98	10.73
Almandine	57.95	59.39	58.75
Spessartine	4.83	1.92	5.99
Grossular	27.71	26.71	24.52

Table 4. CHEMICAL ANALYSES OF INDIVIDUAL MINERAL PHASES IN TYPICAL PELITIC SCHISTS

Specimen	76-462				76-463		
	1	2	3	4	5	6	7
Mineral	Phengite	Biotite	Chlorite	Chlorite	Phengite	Ilmenite	Garnet[1]
SiO_2	51.25	35.61	24.68	24.27	49.48	0.41	36.86
TiO_2	0.70	1.34	0.11	0.18	0.95	57.19	0.13
Al_2O_3	28.22	19.32	23.24	83.15	28.97	0	21.75
Cr_2O_3	0.14	0	0.20	0.17	0	0.22	0.19
FeO	2.54	22.08	27.31	29.44	3.59	41.77	37.76
MnO	0	0	0	0	0	0.30	0
MgO	2.18	7.78	12.93	11.39	2.37	0	2.64
CaO	0.58	0.53	0.09	0	0.50	0.11	0.67
Na_2O	0	0	0	0	0	0	0
K_2O	9.88	9.42	0.06	0.13	9.65	0	0
H_2O	4.52	3.92	11.39	11.27	4.49	0	0
Total	100.00	100.00	100.00	100.00	100.00	100.00	100.00
			STRUCTURAL FORMULAE				
No. Oxygen	22	22	28	28	22	6	12
Si	6.80	5.44	5.19	5.16	6.60	0.02	2.97
Al	1.20	2.56	2.81	2.84	1.40	0	0.03
Σ	8.00	8.00	8.00	8.00	8.00	-	3.00
Al	3.21	0.92	2.96	2.97	3.16	0	2.07
Ti	0.07	0.15	0.02	0.03	0.10	2.11	0.01
Cr	0.01	0	0.03	0.03	0	0.01	0.01
Fe^{2+}	0.28	2.82	4.80	5.24	0.40	1.71	2.55
Mn	0	0	0	0	0	0.01	0
Mg	0.43	1.77	4.05	3.61	0.47	0	0.32
Σ	4.00	5.66	11.86	11.87	4.13	-	-
Ca	0.08	0.09	0.02	0	0.07	0.01	0.06
Na	0	0	0	0	0	0	0
K	1.67	1.84	0.02	0.04	1.64	0	0
Σ	1.75	1.92	0.04	0.04	1.71	-	-
OH	4.00	4.00	16.00	16.00	4.00	0	0

Analyses obtained using a Jeol JX-50A Electronprobe microanalyser at the Central Science Laboratory, University of Tasmania (beam current 15mA, accelerating voltage 15kV).

Analyses of hydrous phases are recalculated on the basis that the structures contain ideal water and all iron is assumed to be in the bivalent state.

Table 4 (continued)

Specimen	76-463					
	8	9	10	11	12	13
Mineral	Phengite edge	Albite*	Altered Biotite	Muscovite	Biotite	Phengite
SiO_2	45.78	67.96	31.72	46.15	34.85	50.21
TiO_2	0.34	0	1.36	0.42	1.01	0.61
Al_2O_3	37.30	19.56	20.06	37.19	19.76	30.00
Cr_2O_3	0.13	0.12	0.17	0.12	0	0.12
FeO	1.44	0	27.66	0.93	24.42	2.42
MnO	0	0	0	0	0	0
MgO	0.56	0	9.36	0.18	6.74	1.79
CaO	0.71	0.11	0.46	0.55	0.47	0.56
Na_2O	0.29	12.17	0	0.78	0	0
K_2O	8.90	0.08	5.34	9.14	8.86	9.76
H_2O	4.55	0.07	3.87	4.55	3.89	4.52
Total	100.00	100.00	100.00	100.00	100.00	100.00
			STRUCTURAL FORMULAE			
No. Oxygen	22	32	22	22	22	22
Si	6.03	11.91	4.91	6.08	5.37	6.65
Al	1.97		3.09	1.92	2.63	1.35
Σ	8.00	-	8.00	8.00	8.00	8.00
Al	3.83	4.04	0.57	3.85	0.96	3.34
Ti	0.03	0	0.16	0.04	0.12	0.06
Cr	0.01	0.02	0.02	0.01	0	0.01
Fe^{2+}	0.16	0	3.58	0.10	3.15	0.27
Mn	0	0	0	0	0	0
Mg	0.11	0	2.16	0.04	1.55	0.35
Σ	4.14	-	6.49	4.04	5.77	4.03
Ca	0.10	0.02	0.08	0.08	0.08	0.08
Na	0.07	4.14	0	0.20	0	0
K	1.50	0.02	1.05	1.54	1.74	1.65
Σ	1.67	-	1.13	1.81	1.82	1.73
OH	4.00	0	4.00	4.00	4.00	4.00

* Orthoclase (mol%) 0.50
Albite 99.00
Anorthite 0.50

Table 4 (continued)

Specimen	76-463	76-443				
	14	15	16	17	18	19
Mineral	Phengite	Garnet[2]	Chlorite	Chlorite	Phengite	Quartz
SiO_2	49.75	38.42	26.25	26.49	47.19	99.71
TiO_2	0.63	0.12	0.15	0	0	0
Al_2O_3	30.26	22.07	20.72	21.37	31.09	0.3
Cr_2O_3	0.10	0.13	0.16	0.10	0.12	0
FeO	2.57	30.32	23.34	20.64	7.05	0
MnO	0	0	0	0	0	0
MgO	2.19	8.36	17.77	19.64	1.36	0
CaO	0.52	0.57	0	0	0.64	0
Na_2O	0	0	0	0	0	0
K_2O	9.46	0	0	0	8.10	0
H_2O	4.52	0	11.60	11.76	4.45	-
Total	100.00	100.00	100.00	100.00	100.00	100.01
			STRUCTURAL FORMULAE			
No. Oxygen	22	12	28	28	22	2
Si	6.59	2.98	5.42	5.40	6.36	0.997
Al	1.41	0.02	2.58	2.60	1.64	-
Σ	8.00	8.00	8.00	8.00	8.00	-
Al	3.32	2.00	2.47	2.53	3.30	0.003
Ti	0.06	0.01	0.02	0	0	0
Cr	0.01	0.01	0.03	0.02	0.01	0
Fe^{2+}	0.28	1.97	4.03	3.52	0.79	0
Mn	0	0	0	0	0	0
Mg	0.43	0.97	5.47	5.96	0.27	0
Σ	4.11	-	12.02	12.03	4.38	-
Ca	0.07	0.05	0	0	0.09	0
Na	0	0	0	0	0	0
K	1.60	0	0	0	1.39	0
Σ	1.67	-	0	0	1.48	-
OH	4.00	0	16.00	16.00	4.00	-

Table 4 (continued)

Specimen	76-462				
	20	21	22	23	24
Mineral	Garnet[3] (rim)	Garnet[4] (core)	Garnet[5] (core)	Garnet[6] (rim)	Garnet[7] (core)
SiO_2	38.81	36.90	36.43	37.2	37.35
TiO_2	0.13	0.13	0.22	0.23	0.18
Al_2O_3	22.05	21.03	20.84	21.18	21.28
Cr_2O_3	0.16	0.23	0.31	0.15	0.18
FeO	31.96	32.59	32.88	38.22	37.80
MnO	0	5.73	6.52	0	0
MgO	6.4	0.32	0	2.49	2.72
CaO	0.49	3.06	2.76	0.55	0.49
Na_2O	0	0	0	0	0
K_2O	0	0	0.07	0	0
H_2O	-	-	-	-	0.18
Total	100.00	100.00	100.00	100.00	100.00
	STRUCTURAL FORMULAE				
No. Oxygen	12	12	12	12	12
Si	3.03	3.01	2.99	3.00	3.01
Al	-	-	-	-	-
Σ	-	-	-	-	-
Al	2.03	2.02	2.01	2.02	2.02
Ti	0.01	0.01	0.01	0.01	0.01
Cr	0.01	0.01	0.02	0.01	0.01
Fe^{2+}	2.09	2.22	2.25	2.58	2.55
Mn	0	0.40	0.45	0	0
Mg	0.74	0.04	0	0.30	0.33
Σ	-	-	-	-	-
Ca	0.04	0.27	0.24	0.05	0.04
Na	0	0	0	0	0
K	0	0	<0.01	0	0
Σ	-	-	-	-	-
OH	-	-	-	-	-

(mol%)	1	2	3	4	5	6	7
Pyrope	9.14	28.47	22.44	1.15	0	8.67	8.79
Almandine	88.95	69.78	76.22	76.59	77.12	89.73	89.91
Spessartine	0	0	0	13.73	15.34	0	0
Grossular	1.91	1.12	1.34	8.53	7.53	1.59	1.29

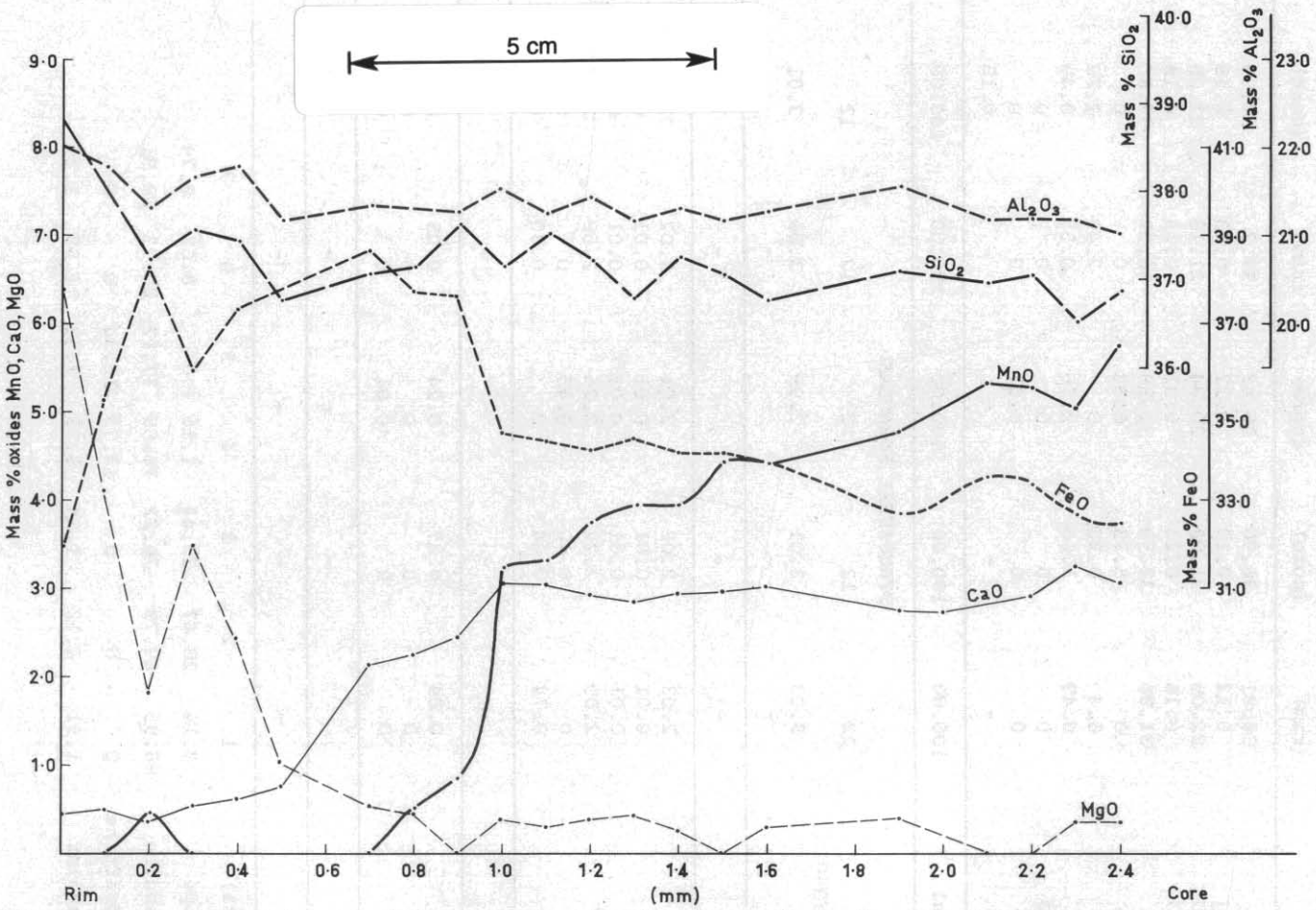

Figure 6. *Zonation pattern in garnet from specimen 76-462 (typical of other specimens analysed). Variation in Ca and Mg contents are very marked. All analyses have been normalised. The sharp break in the MnO curve at 0.1 mm supports the optical evidence that the rim grew separately from the core.*

quartz (type 3 and type 1, as zoisite is not in contact with garnet and phengite) is typical of low grade assemblages. Winkler (1979) argues that the absence of staurolite in such an assemblage means that conditions are below the amphibolite facies. The low Mn content of this garnet implies that the metamorphic pressure exceeded 400 MPa (Hirschberg and Winkler, 1968).

Specimen 76-462 has been analysed in detail and provided mineralogical evidence of two stages of metamorphism, supporting the petrographic implications. Analyses of a large garnet grain (5 mm diameter) at 100 μm intervals are plotted in Figure 6. The garnets are clearly zoned, especially in CaO, MnO, FeO and MgO. MgO and FeO vary sympathetically. There is a clear compositional break in the MnO and CaO contents at 1000 μm from the rim. The pattern of zonation is similar to the 'bell-shaped' curve shown by Råheim (1975) for the CaO profile, but the MnO curve drops dramatically from over 3% to 0% in 30 μm. In addition, individual garnet grains (clear garnet, analyses 23 and 24, table 4) contain no MnO in either the core or the rim. This implies that new crystallisation sites were activated during a second metamorphic event and that either no manganese was available in the vicinity to concentrate in the new garnets, or that temperatures were higher in that event. The old zoned garnets also became nucleation sites during the second event, and the profiles indicate that the mobility of MnO in particular was very limited. The fairly continuous change in the MgO and CaO profiles indicates a situation similar to that proposed by Råheim (1975) of progressive metamorphism, but the different textural positions implies that the growth of the MnO-poor garnet took place after the development of the S_2 foliation. It is probable that the development of S_2 occurred during a plateau of P-T conditions, and that further burial, due to increased load, produced the second, higher temperature metamorphic event which texturally post-dates S_2. Rim effects are not present, although there is a minor anomaly in the curve at 200 μm. The chlorite in this specimen is a magnesium-iron chlorite (Mg value = 0.41 to 0.44). The Si^{4+} content of the phengite (3.4) suggests a temperature of 375°C at 400 MPa (Velde, 1967). This low temperature suggests that the phengite may be a late stage mineral (*cf.* Boulter and Råheim, 1974).

Several minerals have been analysed from specimen 76-463 (table 4) and indicate the complexity of the phyllosilicate geochemistry. The Si^{4+} content of phengite varies from 3.33 to 3.02 within the same thin section. Although zoning of phengite has been established, with analyses 12, 13, 14 (table 4) coming from the same grain, the extreme variation implied by these analyses indicates a wide range in P-T conditions using the curves developed by Velde (1967). The variation in composition from phengite to biotite is optically continuous. The biotite (12) is adjacent to a garnet porphyroblast and is formed by metamorphism of phengite. This is probably the reaction discussed by Thompson and Norton (1970):

[chlorite + muscovite + quartz]
= [almandine-rich garnet + biotite + H_2O]

Because the manganese content of the garnet is very low, as is the grossular component, it is likely that this represents a moderately high pressure (>400 MPa) assemblage. The temperature is probably in excess of 400°C (Si^{4+} content of phengite <3.30), but the exact white-mica composition of the equilibrium assemblage is unknown, as phengite is involved in the garnet forming reaction. Albite has a composition of Ab 99.0, indicating that conditions are too low for the formation of oligoclase. The most likely equilibrium phengite is analysis 13, as this is in contact with the biotite produced during the reaction. This indicates a temperature of

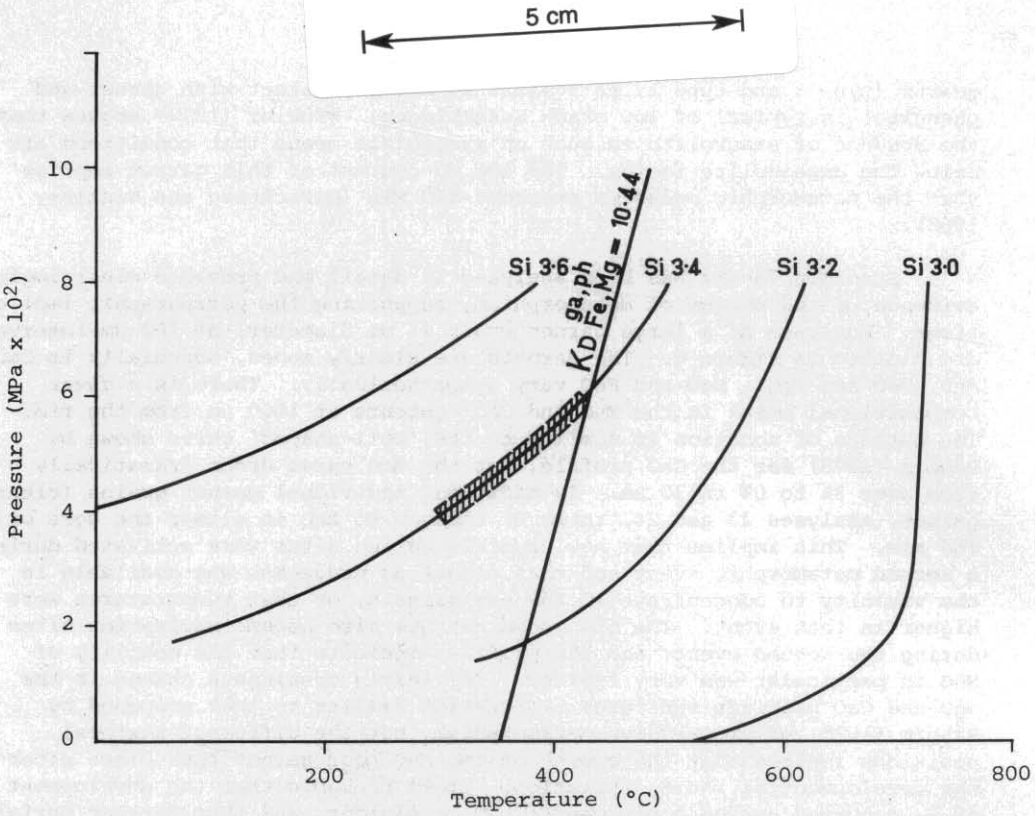

Figure 7. *Pressure-temperature plots of the Si content of phengite (Velde, 1967) and the equilibrium distribution constant K_D of Fe^{2+} and Mg between garnet and phengite from Krogh and Råheim (1978). Phengites with an Si content of 3.3 intersect the K_D line at ≈400 MPa and 400°C.*

400°C at a pressure of 400 MPa. An independent pressure geobarometer is not available, but using the formula of Krogh and Råheim (1978) for a temperature estimate:

$$T(°K) = \frac{3685 + 77.1\ P(Kb)}{\ln K_D + 3.52}$$

$$T(°K) = 628 + 13.145\ P(Kb) \qquad K_D = 10.44$$

This curve intersects the Si^{4+} content = 3.3 curve at about 400 MPa and 400°C (fig. 7), suggesting this as a low P-T limit for the metamorphism. This K_D value does not alter significantly using any of the phengite FeO/MgO ratios. Analysis 10 indicates that biotite is altering to chlorite in this specimen.

DISCUSSION

The chemical and microprobe data indicate that metamorphism is [almandine]-low grade or almandine + chlorite + muscovite zone (Winkler, 1979). Slightly disparate results about pressure-temperature conditions occur when comparing amphibolite and schist assemblages, the former indicating temperatures of between 450°C and 500°C at a pressure of 400 MPa, the latter indicating temperatures of about 400°C and a pressure of about 400 MPa. Insufficient data has been collected to resolve this discrepancy. The spessartine component of garnet from the pelite, and grossular component of garnet from the amphibolite, mean that neither assemblage will fit an ideal system. In

particular the effect of the calcium molecule is unpredictable (Råheim and Green, 1974) and may indicate a higher pressure of metamorphism, or a reduction in the temperature at which the amphibolite assemblage is stable.

TEXTURAL EVOLUTION OF THE PRECAMBRIAN ROCKS

Metamorphic mineral assemblages in the area studied can be divided into garnet-bearing and garnet-free types. The garnet-bearing rocks are geographically restricted to the area west of Payne Bay [DN140080] and surrounding Davey Head [DN084045]. Outside this area, phyllite is glossy and commonly contains small albite porphyroblasts, and albite-bearing muscovite schist occurs. The relationship between the position of garnet-bearing rocks and major structures is not clear, but it seems apparent that the highest metamorphic grade occurred in areas underlain by garnet-bearing rocks. In the Spain Bay area [DN160980], quartz-albite-muscovite schist and chlorite schist suggest that the metamorphic grade may not be very much below the garnet isograd, whereas around Bramble Cove and Coffin Creek the phyllite is fine-grained with only small albite porphyroblasts, and no coarse-grained mica schist has been found. This indicates that the metamorphic grade could be less than in other garnet-free areas.

The mineralogy of the rocks is similar to that found in other metamorphosed Precambrian rocks in Tasmania (Gee, Marshall, and Burns, 1970; Williams, 1971), which have been shown to belong to the greenschist or lower amphibolite facies. The common metamorphic feldspar is albite, and biotite, muscovite, phengite, and garnet are the other common minerals present. In amphibolite, epidote and garnet co-exist with actinolite or hornblende, as well as oligoclase and chlorite, a low-grade higher temperature amphibolite assemblage (Winkler, 1979). There is considerable variation in metamorphic assemblages in Tasmania. Whereas biotite is common at Port Davey, very little biotite is present in the Mt McCall area (Williams, 1971) or in the Strathgordon area (Boulter, 1978). The garnet-bearing rocks around Trumpeter Islets [DN035072] appear to be unique in the size of garnet (up to 15 mm) and albite (up to 30 mm) porphyroblasts formed.

RELATIONSHIP BETWEEN MINERAL GROWTH AND STRUCTURAL EVENTS

Garnet is poikiloblastic, containing numerous inclusions of quartz in trails. It is usually subhedral to euhedral, pink in colour, and strongly zoned. The common size of garnet is about 10 mm. The dominant cleavage in the rocks (*e.g.* 76-445) is a differentiated crenulation cleavage. Lozenges of quartzite contain a preserved fabric discordant with the dominant cleavage, and this is referred to as S_1. The dominant cleavage is S_2. Garnet porphyroblasts consist of euhedral centres containing inclusion trails, surrounded by rims containing many dispersed inclusions, aligned in a similar direction to those in the core. The S_2 surface is deflected around the garnet rims and pressure shadows have formed behind the garnet, extending out to the rim. This indicates that garnet centres and rims grew prior to the formation of S_2, and that rim growth differed from the growth of the garnet core. Because S_1 is only preserved as slightly curved inclusion trails, the core of the garnet must have formed synchronously but late in D_1. The rims also show discordance between S_i and S_2, and therefore crystallised prior to the D_2 event, but also formed later than the D_1 event. The conclusion from these textures is that two metamorphic events occurred prior to the second deformation event.

Albite crystals are untwinned and contain garnet without rims and with inclusion trails, which suggests that albite grew during the same metamorphic event which produced garnet rims. The albite also contains

concordant inclusion trails of muscovite, biotite, and chlorite and is folded with S_2 around garnet crystals. It is elongated parallel to the S_2 cleavage, and has cleavage-parallel grain boundaries against muscovite. It is concluded that the albite is dominantly synchronous with S_2. When the albite is porphyroblastic, S_2 mica grains abut the grain boundaries with minor deflection, and biotite in particular tends to replace the albite. This suggests that biotite crystallised during D_2 and that albite began crystallising just prior to the formation of biotite and muscovite during D_2. The albite attained its present size prior to the S_3 cleavage.

In other rocks the albite is porphyroblastic, shows simple twinning (76-501), and S_2 is partially dispersed around the crystals. S_e and S_i are discordant and indicate a pre-D_2 albite growth. Other albite crystals in the same rock show concordant, straight inclusion trails showing growth during or after D_2. This later albite is euhedral. Discordant helicitic structures in albite (76-486) show pre-D_2 albite growth. In this sample, albite laths show multiple twinning and have pressure shadows associated with S_2. Garnet is in small, rounded, inclusion-free grains which overgrow all other mineral phases, indicating post D_2 metamorphic growth. Garnet of this age is also present in 76-478. The metamorphic history of the region is therefore complex, with albite and garnet textures indicating different growth histories in relation to deformation over small areas.

Biotite is a common constituent of most garnet-bearing schist, forming large flakes aligned in the D_2 direction. Small biotite inclusions in D_2 albite indicate the pre-existence of biotite, probably associated with the early growth of garnet. Muscovite also crystallised during D_1 and D_2, as it defines an early foliation (S_1) in quartzite lozenges preserved in S_2, and forms grains similar in size and shape to biotite. Muscovite grew during the D_3 event in sample 76-478, and is intergrown with a garnet crystal. The muscovite assumes biotite characteristics in the garnet crystal, proving that the local availability of ions largely controlled mineral growth during D_3, and diffusion was minor. The muscovite grains in schist show simple twinning. In 76-443 there are two optically distinct muscovite populations, with muscovite occurring in small grains in discrete lozenges (uniaxial), which also contain zoisite, and also as large fresh grains which have a biaxial negative character.

Chlorite is in two forms, a pale green pleochroic variety with brownish or grey interference colours, and another a darker green colour in polarised light, but with anomalous blue interference colours. Chlorite in pressure shadows associated with the D_2 cleavage is in the form showing brown or grey interference colours and is probably the product of prograde metamorphism. The chlorite with anomalous blue colours is secondary, forming after garnet and biotite during a retrograde metamorphic event. However in specimen 76-443 the chlorite with brownish interference colours contains small allanite grains with pleochroic haloes. It is difficult to realise this situation in a chlorite lattice, and the observation suggests that the grey chlorite in this rock is secondary after biotite. The age of the alteration is not certain, but it could represent a P/T metamorphic plateau after D_2, with newly formed biotite retrogressing to chlorite. The phase of metamorphic regression producing the blue chlorite may be later, or else the chlorite may differ because of the different host chemistry being altered (biotite or garnet).

Epidote-bearing garnet albite muscovite schist shows a different textural history. Specimen 76-443 contains anhedral to subhedral garnet replaced by brown birefringent chlorite, which also grows in pressure shadows. Thus M_2 was below the maximum grade of M_1 in these rocks. Muscovite in this

sample occurs as discrete crystals and in lozenges containing stubby, altered 3T muscovite grains and zoisite crystals. The zoisite is associated with M_1 metamorphism, along with muscovite and garnet, because it only occurs in association with lozenges of earlier muscovite. Epidote grains are eroded by biotite crystals and appear to be early metamorphic minerals in 76-488. Albite porphyroblasts contain skeletal garnet and normal garnet inclusions. The texture suggests that garnet, epidote, and biotite formed during an early event, and biotite and albite formed during a later metamorphic period.

Quartz inclusions in both albite and garnet are smaller than the quartz in the rock groundmass. It is inferred that the grain size of quartz increased during the second metamorphic event. However in quartzite, the fabric diagrams from the adjacent Bathurst Quadrangle (Williams, 1979) show a strong preferred orientation of quartz grains; the analysis of a quartz vein in the quartzite showed an identical fabric. This suggests that the grain size characteristics of typical quartzite are a secondary metamorphic feature and were not associated with dynamic processes. The conclusion drawn from this is that quartz recrystallisation during M_2 was in a static environment. Dynamic crystallisation of muscovite in the S_2 direction produced grain boundary alterations in the quartzite, but did not produce major quartz optic axis fabric changes.

This situation is entirely different to the fabric behaviour in quartzite in central Tasmania. Williams (1971) showed that quartz optic axis fabric changes were pronounced during the second structural event, changing girdle fabrics into near point maxima optic axis fabrics. This factor, with only one major structural/metamorphic event causing optic axis orientation, explains to a large degree the poor re-orientation of quartz axes in some areas (*e.g.* Bramble Cove), as only one event need be of lower intensity or the deformation of one event may be taken up by less competent rock units.

At Spain Bay and north of Coffin Creek, no garnetiferous rocks have been found. Assemblages are normally phengite-chlorite-quartz-biotite and phengite-chlorite-albite-biotite-quartz. Albite contains helicitic inclusion trails (76-516, 76-467) which are strongly discordant with the surrounding crenulation cleavage. Quartz-chlorite pressure shadows have also formed around the albite laths. There are well crystallised muscovite flakes parallel to the crenulation cleavage (S_2), but chlorite and biotite are commonly truncated by S_2. These relations show that the early metamorphic peak (M_1) produced biotite and albite. The age of the chlorite (anomalous interference colours) is uncertain, as it also occurs in pressure shadows, apparently associated with S_2. The formation of albite synchronously with D_1 is implied by the sigmoidal form of inclusion trails. The S_3 surface is a spaced crenulation cleavage formed by the concentration of opaque material in the limbs of small scale (<10 mm) folds in the earlier crenulation cleavage. It was not associated with extensive mineral growth. Phyllite without albite (76-514) has finer grained muscovite and chlorite growing parallel to the S_2 crenulation cleavage. Muscovite and quartz crystals preserved in microlithons formed during an earlier metamorphic event, the muscovite defining S_1. An S_3 crenulation cleavage is also developed.

SUMMARY

Metamorphism at Port Davey took place during three episodes. The earliest metamorphic event resulted in the formation of garnet, zoisite, biotite, and muscovite in the rocks. Textural evidence of straight to very

Plate 1. *Sedimentary flame structures preserved in fine-grained quartzose rocks from Wallaby Bay.*

Plate 2. *Possible 'mudstone' flakes preserved in the layer below the scale in Plate 1. Scale divisions are 10 mm.*

slightly curved discordant inclusion trails in garnet shows that metamorphism was synchronous with the first deformation event. The second metamorphic event in garnet-bearing rocks produced garnet rims which are optically distinct from the cores. The rims also contain discordant inclusion trails, more numerous inclusions, and the S_2 crenulation cleavage warp around them, indicating that the rims formed prior to S_2. The first metamorphic event only produced zoisite and biotite in rocks of suitable composition. The second metamorphic episode may have caused retrogression of biotite to chlorite, as chlorite with allanite inclusions occurs in some specimens.

Following these two pre-D_2 metamorphic events, chlorite formed from retrogression of garnet and biotite, and muscovite grew during later deformation events. The metamorphic mineralogy varies over the area, and the absence of garnet in biotite-albite phyllite around Spain Bay and Coffin Creek suggests that the metamorphism is zoned.

STRUCTURAL GEOLOGY

The Precambrian rocks in the quadrangle have been deformed during five deformation episodes, which produced characteristic mesoscopic and macroscopic structures. The major distribution of rock types is controlled by the second and third deformation events; structural profiles showing this distribution are included on the map sheet.

Despite the complex deformation history, an isolated area showing primary sedimentary structures is preserved on the coast at Wallaby Bay [DN156070], where ball and pillow structures and load structures are preserved in fine-grained quartzose beds. Their irregular form, and the deformation of the laminae in the coarser grained layers in a sympathetic manner, indicates that these are not tectonic boudinage structures (plates 1, 2). In general, the deformation intensity and transposition structures associated with early folding obliterates the primary sedimentary features. Plates 3 and 4 show remnant fold cores which formed during the earliest deformation event in quartzite sequences. Both folds are partly boudinaged. Truncation of the limbs of these folds is common, showing that large scale translation has occurred parallel to the axial surface of the earliest folds. The scale of this layering is variable. At Berry Head [DN155076] the layering developed is from 200 mm to 500 mm thick, but some layers wedge out at a low angle as a result of the lateral translation of very tight folds. The movement zones are often the site of intense deformation, as evidenced by quartz veins which have been folded and rodded. The presence of linear structures in these zones is characteristic of lateral translation. A typical example of this large scale layering with remnant lamination preserved between translation zones is shown in Plate 5. In phyllite and schist sequences the earliest folds are strictly isoclinal and intensely flattened. The strewn-out fold limbs form the dominant layering in the rock, which is parallel to the fold axis surfaces. These structures are well exposed at South East Bight [DN068050, plate 6]. The cleavage associated with all of these early fold and fault structures is a penetrative fabric consisting of a near perfect alignment of white-mica flakes and a dimensional and crystallographic alignment of quartz grains.

The second deformation event produced the major outcrop patterns in the Spain Bay and Davey Head areas. Plate 7 shows the effect of the interference of F_1 and F_2 folds in a part of the section which behaved in a ductile manner. In quartz-schist and schist regions, the dominant layering is parallel to S_2. The S_2 cleavage is at a low angle to S_1 and is a strongly differentiated asymmetric crenulation cleavage. Plate 8 shows the effect of this low angle crenulation on a thinly laminated quartzose sequence.

Plate 3. *Partly boudinaged isoclinal fold core preserved in pure quartzite. Dominant layering is now parallel to a well-defined axial surface cleavage related to these folds. Cross-cutting cleavage visible in the core area is S_3. East of Toogee Head [DN064068].*

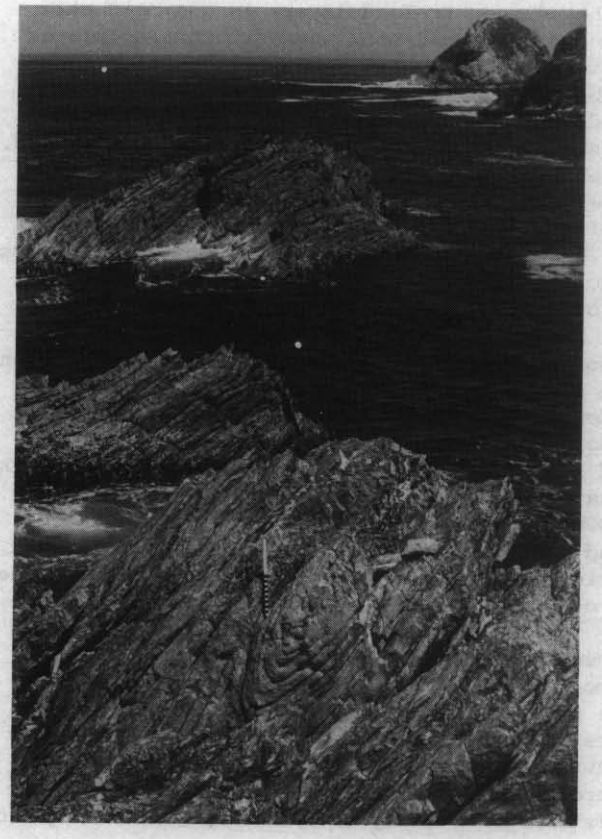

Plate 4. *Boudinaged isoclinal fold core, interpreted as an F_1 fold, in quartz from opposite Trumpeter Islets [DN041071]. Scale is divided into 10 mm intervals.*

Plate 5. *Large scale mechanical layering in quartzite at Berry Head [DN155076]. The oblique surfaces preserved between zones of intense deformation are parallel to the S_1 cleavage and represent preserved F_2 fold limbs.*

Plate 6. *Sequence of well-developed, strictly isoclinal, strongly flattened folds formed during the first deformation event. In thicker layers (top centre) fold cores are preferentially thickened and then boudinaged, resulting in lenticular cleavage structures. South East Bight [DN068050].*

Plate 7. *'Mushroom' type of interference effect between F_1 and F_2 structures at South East Bight. Scale divisions are 10 mm. This interference pattern is not repeated on a regional scale [DN068050].*

Plate 8. *S_2 surfaces cross-cut the well developed S_1 lamination at a low-angle, producing tight folds with axial surfaces sub-parallel to S_1 (centre right) in finely laminated horizons and open asymmetric S-folds in thicker layers. The cleavage development is associated with thickening of the quartzite layer in the F_2 fold cores. Cleavage is much more intense than suggested by the form the folds in thicker layers. Coffin Creek [DN163079].*

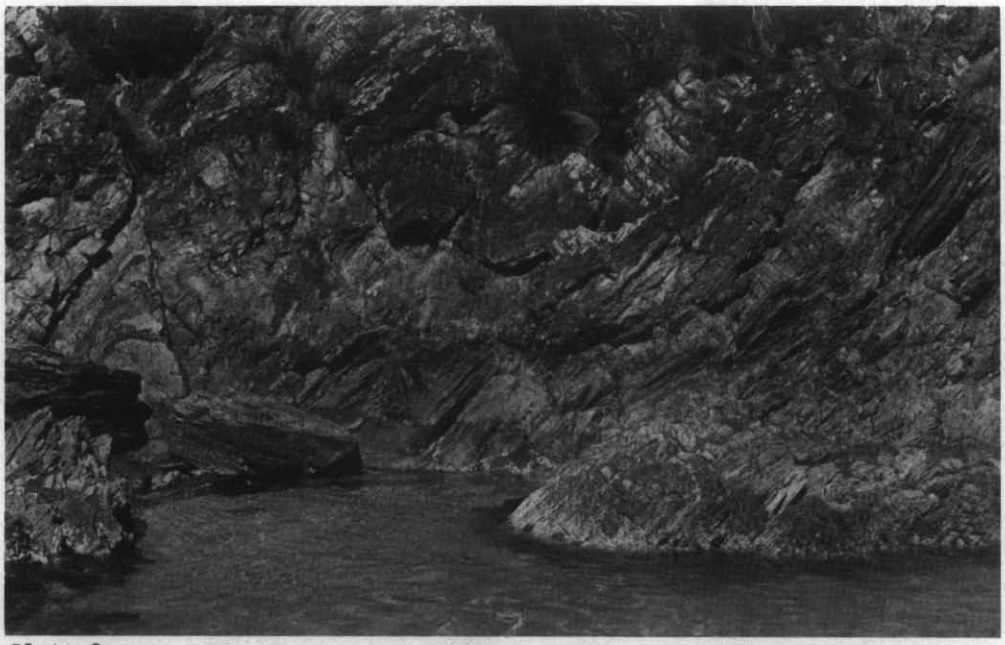

Plate 9. *Typical asymmetric F_3 folds, producing a weak but pervasive cleavage. South East Bight [DN063059].*

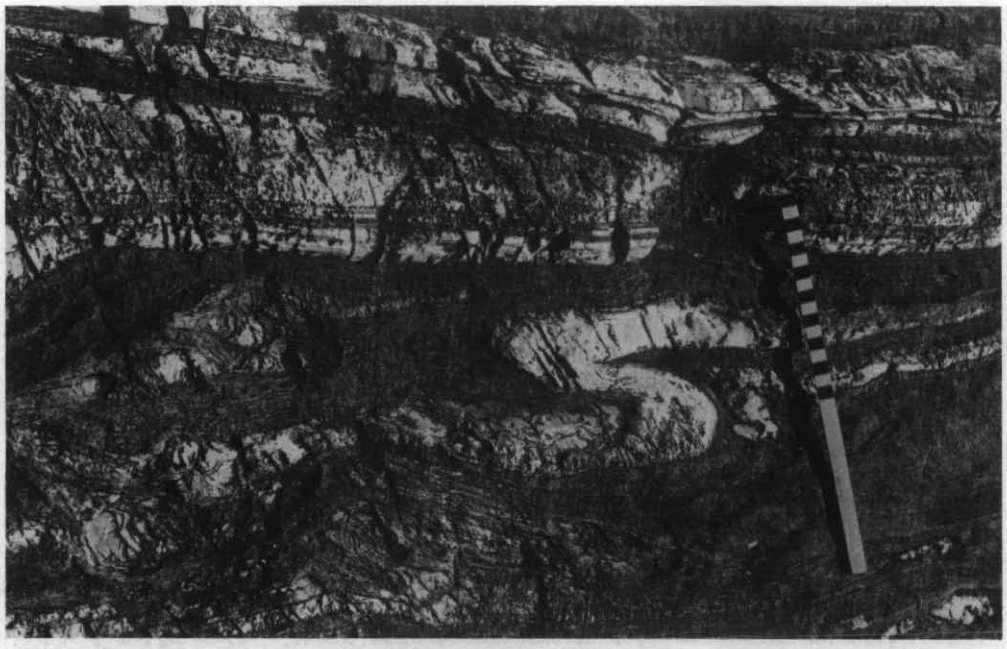

Plate 10. *Form of the fracture cleavage associated with folds which rotate F_3 structures. The fold in the photograph is probably an F_2 structure. North-west of Saddle Bight [DN104506].*

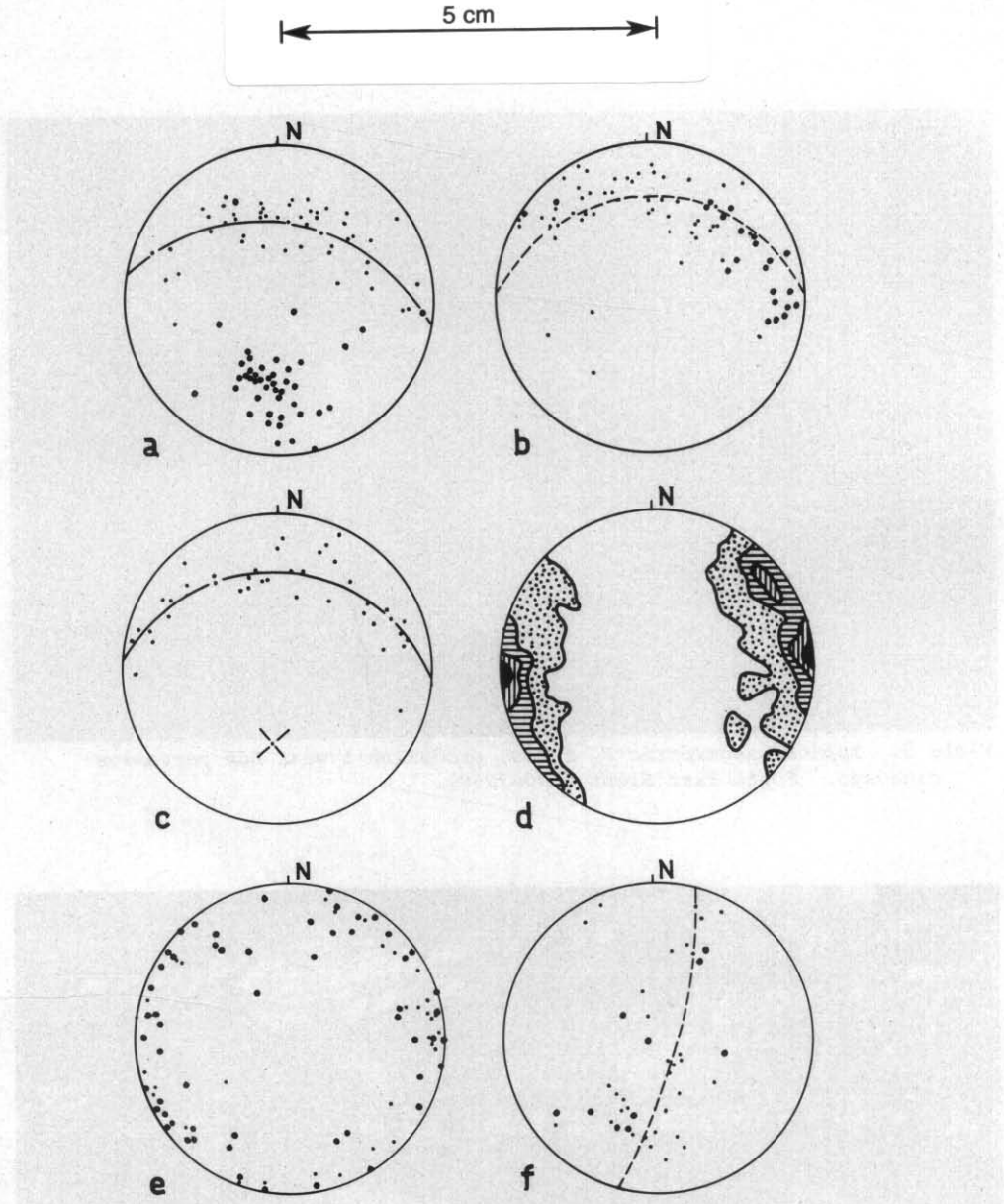

Figure 8. *Orientation data; Spain Bay, Davey Head, and Coffin Creek areas*

(a) 48 poles to layering (.) and 47 fold hinge directions ( ) from the Coffin Creek area. Average fold hinge plunges 45° to 195°.

(b) Poles to layering from Davey Head (.) and South East Bight [DN068050] ( ). Average fold hinge plunges 50° to 186°.

(c) 40 poles to layering from the Spain Bay area. Average fold hinge plunges 50° to 183°.

(d) 122 S_3 cleavage readings from the Spain Bay area, contoured 0.4, 2.0, 4.5, 8.5, and 12.0% per 1% area.

(e) Poles to late cleavages in the Davey Head area. (.) = S_4, ( ) = S_5. These may represent conjugate cleavages.

(f) F_3 and F_4 fold hinges in the Spain Bay area. 46 values.

The layering parallel to S_2 formed dominantly by differentiation on S_2. The regional fold pattern of D_2 structures is indicated on the map sheet. The F_2 folds are reclined to recumbent structures with half wave lengths of about 0.5 km. Mesoscopic folds are asymmetric S and Z folds of low to moderate dihedral angle (20°-60°).

Folds and cleavage developed during later deformation events are common. The layering has generally been folded into moderately tight, flattened flexural slip folds which plunge from 40° to 70° to the SSW. Stereographic projections of data from Coffin Creek (fig. 8a), Davey Head (fig. 8b), and Spain Bay (fig. 8c) all indicate a similar statistical fold hinge direction. The cleavage associated with this event is steeply dipping and trends north-south (fig. 8d). These folds are related to the third major deformation event. The typical mesoscopic form of these folds is shown in Plate 9.

Superimposed on this event are a number of cleavage and fold structures. Profile A-B on the map sheet shows the form of conjugate folds which are co-axial with F_3. A fracture cleavage (plate 10) has developed which is often closely parallel to the S_3 direction, and another surface has developed on a WNW trend which is probably the conjugate direction to the other. The orientation of these two surfaces in the Davey Head area is shown in Figure 8e. Variation in F_3 fold hinge directions has been caused by these later folds. In the Spain Bay area, F_3 fold hinges have been rotated on two hinge-line directions (fig. 8f), indicating folds in a NNE direction and a WNW direction.

FAULTS

Large faults which post-date the D_3 deformation event are present in the region. Their relationship to later deformation events is not established. The fault extending from Spain Bay to Fire Hill [DM142971] has an associated well developed resilicified fault breccia, in a zone up to 30 m wide. The fragments in the breccia contain disoriented S_1 and S_2 cleavage surfaces. The fault displaces D_3 structures. Formation of fault breccia and its silicification suggests that the faults are pre-Tertiary, possibly Devonian structures. The outcrop pattern showing the displacement of the D_3 synform at Coffin Bay shows that there was significant sinistral strike-slip movement on the faults. At Mt McCall (Williams, 1971) transcurrent faults with associated fault breccias were related to the formation of Devonian conical folds, and similar structures in the Davey Quadrangle may also have a Devonian component to their movement. Williams (1979) suggested that the Coffin Bay faults may have operated during late Precambrian times.

JURASSIC(?) DOLERITE

Specimen 76-506 is representative of a medium-grained, blue-grey, equigranular, intermediate igneous rock which occurs as a train of large boulders on the foreshore at DN124066. In thin section, the rock is composed of plagioclase, clinopyroxene, mesostasis, olivine, opaque minerals, and biotite. It is equigranular with a sub-ophitic texture. The feldspar laths are approximately one millimetre long. The maximum extinction angle (32°) indicates a composition of An56. Some feldspar crystals form in a rosette pattern. The intergrown clinopyroxene has a pale pinkish colour, indicating a moderate titanium content. Plagioclase makes up about 50% of the rock, with about 30% clinopyroxene. The mesostasis is very pale green with grey interference colours, and constitutes about 15% of the specimen. Biotite is present as short crystals in the mesostasis. Olivine,

Plate 11. *Silica-cemented, poorly sorted deposits from Bond Bay [DN102111]. These may represent the base of slope (talus) deposits accumulating at sea level.*

Plate 12. *Silica-cemented gravel deposits underlying the breccia shown in Plate 11 [DN113111]. These outcrops reach 18 m above sea level.*

with a diameter up to 1.2 mm, constitutes less than 2% of the rock and has reaction boundaries with the other minerals. Opaque grains make up the remainder of the rock. The intrusion may be representative of either the Tertiary or Jurassic tholeiite suites.

CAINOZOIC DEPOSITS

The Cainozoic deposits are varied, reflecting the influence of changing sea level and climate throughout the era. Talus deposits resting on eroded gravel beds suggest that there is a division of the deposits into two parts. The age of this erosional surface has not been determined, but the talus was probably deposited late in the Last Glacial period. As such, the surface is probably close to the Pleistocene/Holocene boundary.

SILICEOUS CONGLOMERATE (Qpc)

Well cemented siliceous conglomerate beds are exposed south of Coffin Creek [DN165073] and in the north-west corner of Bond Bay [DN113111], just north of the quadrangle boundary. The beds are composed of angular blocks of quartzite and quartz schist up to 260 mm in diameter, in a fine sand sized matrix (ϕ = 3.5). Bedding is preserved in the Bond Bay deposit, with a dip of 5° toward 260°. The bedding is horizontal at Coffin Creek. The nature of the deposit is shown in Plate 11. The coarse grained beds are poorly sorted and show imbrication. The finer beds (plate 12) are structureless, continuous framework fine-conglomerate with moderate sorting. The clasts have a low rounding.

The direction of imbrication in the Bond Bay deposit varies from 060° at the top of the exposures to 270° lower down. The rocks crop out up to 18 m above the present sea level and extend down to sea level. At Bond Bay, the conglomerate at sea level is ferruginous. The conglomerate appears, in both areas, to be restricted to the banks of the river valleys. Transport must have been negligible, because the rounding is so poor, and the presence of an initial dip in the Bond Bay rocks suggests that the material accumulated at the base of a scarp. The imbrication and bedding implies that this scarp was at the back of a beach where partial reworking of the material occurred.

These deposits have been cut by the present river valleys (plate 13). The creeks currently occupying these valleys would be incapable of creating the valleys, which implies that the cemented conglomerate was deposited prior to this erosion, when water discharge was much greater than at present. This suggests that the deposits are older than the Last Glacial period, and the heavily cemented nature of the deposits may indicate a Tertiary age.

RAISED BEACH DEPOSITS OF BEDDED PEBBLES AND COBBLES (Qpb)

These deposits are present on the eastern end of Noyhener Beach [DM186935], at Hannant Inlet [DM188974], Coffin Bay [DN167084], Bond Bay [DN108101], and Cockburn Cove [DN082092]. The deposits rest unconformably on the Precambrian substrate, and occupy a position from 1.5 m to 3.5 m above present sea level. All exposures occur on the present coast line.

At Cockburn Cove and Bond Bay, the deposits occupy the lower topographic level, cropping out at the back of the present beach. The maximum grain size is variable, ranging from 300 mm in some deposits down to 10 mm in others. The grains are dominantly quartzite, of variable shape and moderate roundness. Oblate clasts are aligned horizontally with the long axes plunging towards the present coast line at about 6°.

Plate 13. *Broad, flat-bottomed valleys containing very small present day creeks. The hill on the right-hand side of the valley is composed of silicified conglomerate and breccia beds [DN113111].*

Plate 14. *Cobble horizon directly overlying phyllite at Cockburn Cove [DN082092]. This horizon is separated from the next cobble horizon by a palaeosol.*

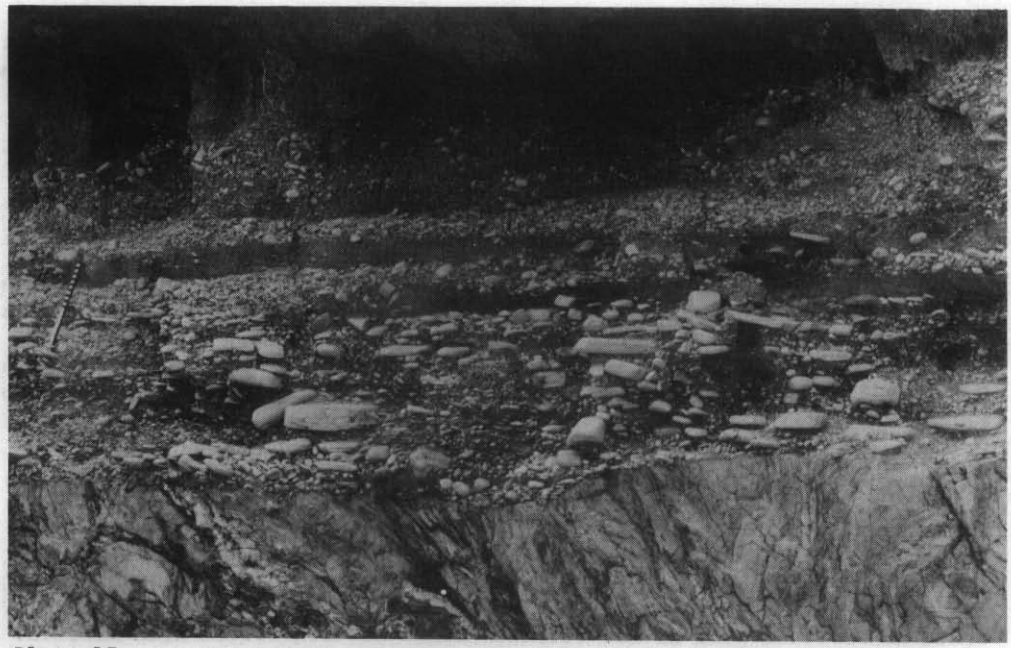

Plate 15. *Bedded cobble deposits at Coffin Bay [DN167084].*

Plate 16. *Bedded cobble deposits cut by an erosional surface overlain by breccia deposits. The breccia deposits are now stabilised and heavily vegetated. Coffin Bay [DN167084].*

At Cockburn Cove, there are two coarse clastic horizons separated by a palaeosol which is about 50 mm thick. The total exposed thickness is one metre (plate 14). The soil horizon is exposed at DN083094 and contains charcoal derived from burnt logs. The lower unit extends below current beach level. At Noyhener Beach, the quartz and quartzite boulders reach 300 mm in diameter and form deposits at least 1.8 m thick. They are overlain by 240 mm of soil with charcoal fragments. The soil horizon is conformably overlain by vegetated dune sand, and is therefore older than the stabilised dunes. The gravel has a sandy matrix and an imbricate texture, and probably correlates with the lower unit at Bond Bay. The gravel at Hannant Inlet is 1.4 m above the present beach deposits, and is well bedded and well sorted in a dark brown muddy silt matrix. Scours are filled with material coarser than the bulk of the deposit, suggesting that reworking of the deposits occurred. At DM188974 (Hannant Inlet) the deposits commence two metres above the beach and are 10 m thick. These are also inferred to be beach deposits, because of the well bedded imbricate nature and their relationship to the present coast line.

The deposits are well exposed in wave-cut platforms at Coffin Bay (plates 15, 16). They commence 1.5 m above the present beach level and lie on an erosional surface on phyllite, and consist of layers of aligned pebbles and cobbles separated by pebbly sand horizons (plate 15), which are poorly sorted polymodal deposits. The phyllite in cliff exposures contains isolated pods of sub-circular cross section filled with breccia. These deposits are interpreted as fossil sea caves, of the same age as the beach deposits. They occur up to four metres above sea level.

OLDER ALLUVIUM (Qpt)

The beach deposits at Coffin Bay are truncated by an erosional surface (plate 16) above which breccia has been deposited. The breccia is composed of angular quartz and quartzite fragments in a sandy matrix. The breccia is in turn overlain by well bedded pebbly sandstone beds related to an old river system, as the beds are eroded by the present creeks and the dip of the pebbles is towards the channel axis.

Both the older alluvium and the raised beach deposits are eroded by another breccia unit, which consists of angular schist and phyllite blocks in a soil matrix. This is interpreted as an old talus deposit, as it is now thickly vegetated and inactive. It most likely formed by periglacial activity during or soon after the Last Glacial period, implying that the raised beach and older alluvial deposits were formed before the Last Glacial period and are therefore most probably Pleistocene in age.

STABILISED DUNE SAND (Qds)

Extensive stabilised sand dunes occur east of Chatfield Point [DM180940], with smaller dune fields behind Spain Bay [DM167976], Bond Bay [DN120086], Kathleen Island [DN175042], and Lourah Island [DM182995]. The dunes reach 25 m in height and have extensive, well developed dune ridges which generally trend in a WNW direction. They overlie the raised beach deposits at Noyhener Beach and are deflated and overridden by currently active sand dunes behind Stephens Bay and Noyhener Beach. The dunes are characteristically vegetated and have a well developed soil profile (a podzolic soil profile about 4 m deep occurs in places). The dunes are longitudinal, as opposed to the transverse present-day back-beach dunes, and were therefore formed during a period of higher average wind speed and greater sand supply than that currently available. In comparison to similar relationships in north-east Tasmania (Baillie *in* McClenaghan *et al.*, 1982),

it is inferred that the dunes were probably formed during the Last Glacial sea level low, and hence are probably Pleistocene in age.

TALUS (Qt)

Talus has formed on and at the foot of the slopes of most major quartzite ridges and locally on the coast line (*e.g.* Coffin Bay, see above). The talus slopes are now vegetated and have a sandy soil matrix. Quartzite forms the dominant component of the talus fields, although local coastal talus deposits contain schist and phyllite blocks. The quartzite blocks are usually up to 300 mm in diameter and partly rounded, the rounding occurring during the downslope movement. It is probable that these slope deposits formed during a previous cold climatic period with little vegetation cover. They are therefore Last Glacial in age at the latest, but could in part be reworked (by solifluction) older slope deposits. They therefore represent deposits formed close to the Pleistocene/Holocene boundary (Colhoun, *in* Leaman, 1977).

Deposits which are younger than the talus deposits are recognised by being directly related to the current sea level and drainage systems. The age relationships between these Holocene deposits is unclear, but some are certainly contemporaneous. No detailed work has been attempted.

TIDAL FLAT DEPOSITS AND MUD BANKS (Qm)

Extensive tidal flat deposits have developed in Kelly Basin [DN100080] and Hannant Inlet [DM185960]. The thickness of the deposits is unknown. Both Kelly Basin and Hannant Inlet are large bodies of water with a narrow entrance to the sea, and the silt and mud of the tidal flats have undoubtedly been deposited as a result of flocculation due to the mixing of fresh water and the tidal salt water. The absence of strong current circulation in these basins results in the absence of abundant sand horizons.

Estuarine mud banks have formed in Coffin Creek [DN163074], probably as a result of flocculation where the salty estuarine waters mix with the fresh sediment-rich water of Coffin Creek.

BEACH SAND AND COBBLE DEPOSITS (Qb)

Sand beaches have formed in the large bays on most of the unexposed coast line, the beaches at Stephens Bay and Noyhener Beach being the most extensive. The sand has accumulated by longshore drift from the adjacent headlands. The majority of the coast line, however, is rocky, reflecting the very high wave energy produced by the prevailing westerly winds and the very deep offshore waters (*e.g.* 26 m depth 100 m south of Point Lucy, average 20 m depth 500 m offshore around the Davey Head coast line).

Cobble beaches have formed by the coastal erosion of Pleistocene cobble beaches (Qpb) in places around Kelly Basin and Coffin Bay, and are usually very narrow. In places these cobble deposits have been lithified by a ferruginous cement (Qbf). It is suggested that acidic groundwater rich in iron has deposited the iron on the beach as a result of mixing with salt water. Similar ferruginous conglomerate occurs on the beaches around Bathurst Harbour.

MOBILE DUNE AND BLOWN SAND (Qd)

Sand dunes up to 40 m high have formed behind Stephens Bay and Noyhener Beach. They are unvegetated and actively encroaching over the

stabilised dunes. The dune ridges are short, but trend parallel to the current beaches.

ALLUVIUM AND SWAMP DEPOSITS (Qa)

Currently active creeks in the Davey Quadrangle occupy low lying areas with broad flat valleys. These areas are filled with pebbly sand deposits which form a veneer over the flatter areas. They are probably not very thick, rock outcrop usually commencing at any topographic irregularity. However west of Kelly Basin [DN075076], there are terraces up to 500 m from the present creek at heights of about 5 m above the present drainage level. These indicate previous higher river levels and any deposits on and related to these terraces may be of a similar age to the talus deposits, or only slightly younger.

Many of the areas covered with Holocene alluvium are now button grass plains.

REFERENCES

BOULTER, C.A. 1978. *The structural and metamorphic history of the Wilmot and Frankland Ranges, south-west Tasmania*. Ph.D. thesis, University of Tasmania : Hobart.

BOULTER, C.A.; RÅHEIM, A. 1974. Variation in Si^{4+}-content of phengites through a three stage deformation sequence. *Contr.Miner.Petrology* 48:57-71.

de WIT, M.J. 1976. Metamorphic textures and deformation : A new mechanism for the development of syntectonic porphyroblasts and its implications for interpreting timing relationships in metamorphic rocks. *Geol.J.* 11:71-100.

ESKOLA, P. 1939. Die metamorphen gesteine, *in* BARTH, T.F.W.; CORRENS, C.W.; ESKOLA, P. *Die entstehung der gesteine*. Springer : Berlin. 263-407.

EVERARD, G. 1961. Notes on specimens collected in various localities. Port Davey district. *Tech.Rep.Dep.Mines Tasm.* 5:206-208.

GEE, R.D.; MARSHALL, B.; BURNS, K.L. 1970. The metamorphic and structural sequence in the Precambrian of the Cradle Mountain area, Tasmania. *Rep.geol.Surv.Tasm.* 11.

HIRSCHBERG, A.; WINKLER, H.G.F. 1968. Stabilitätsbeziehungen zwischen chlorit, cordierit und almandin bei der metamorphose. *Contr.Miner. Petrology*. 18:17-42.

HOSCHEK, G. 1969. The stability of staurolite and chloritoid and their significance in metamorphism of pelitic rocks. *Contr.Miner.Petrology*. 22:208-232.

KEID, H.G.W. 1944. Geological report on Port Davey area. *Unpubl.Rep.Dep. Mines Tasm.* 1944:31-33.

KROGH, E.J.; RÅHEIM, A. 1978. Temperature and pressure dependence of Fe-Mg partitioning between garnet and phengite, with particular reference to eclogites. *Contr.Miner.Petrology*. 66:75-80.

LEAMAN, D.E. 1977. Geological atlas 1:50 000 series. Sheet 75(8312N). Brighton. *Explan.Rep.geol.Surv.Tasm.*

McCLENAGHAN, M.P.; TURNER, N.J.; BAILLIE, P.W.; BROWN, A.V.; WILLIAMS, P.R.; MOORE, W.R. 1982. Geology of the Ringarooma-Boobyalla area. *Bull. geol.Surv.Tasm.* 61.

PAPIKE, J.J.; CAMERON, K.L.; BALDWIN, K. 1974. Amphiboles and pyroxenes : Characterization of other than quadrilateral components and estimates of ferric iron from microprobe data. *Geol.Soc.Am.Abstracts with Programs.* 6:1053-1054.

RÅHEIM, A. 1975. Mineral zoning as a record of P, T history of Precambrian eclogites and schists in western Tasmania. *Lithos* 8:221-236.

RÅHEIM, A.; GREEN, D.H. 1974. Talc-garnet-kyanite-quartz schist from an eclogite-bearing terrain, Western Tasmania. *Contr.Miner.Petrology.* 43:223-231.

SCOTT, J.R. 1876. Port Davey in 1875. *Pap.Proc.R.Soc.Tasm.* 1875:94-107.

SPRY, A.H.; BAKER, W.E. 1965. Precambrian rocks of Tasmania, part VII. Notes on the petrology of some rocks from the Port Davey-Bathurst Harbour area. *Pap.Proc.R.Soc.Tasm.* 99:17-26.

STEFANSKI, M.Z. 1961. Denison copper prospects - western Port Davey. *Tech.Rep.Dep.Mines Tasm.* 5:60-62.

THOMPSON, J.B.; NORTON, S.A. 1970. Paleozoic regional metamorphism in New England and adjacent areas, *in* ZEN, E-an; WHITE, W.S.; HADLEY, J.B. *et al. Studies of Appalachian geology, northern and maritime.* Interscience : New York. 319-327.

VELDE, B. 1967. Si^{+4} content of natural phengites. *Contr.Miner.Petrology.* 14:250-258.

WILLIAMS, P.R. 1971. *Petrology and structure of the Mt McCall area.* B.Sc. Hons. thesis, University of Tasmania : Hobart.

WILLIAMS, P.R. 1979. *Basin development, environment of deposition and deformation of a Precambrian(?) conglomeratic flysch sequence at Bathurst Harbour, S.W. Tasmania.* Ph.D. thesis, University of Tasmania : Hobart.

WINKLER, H.J.F. 1979. *Petrogenesis of metamorphic rocks (5th ed.)* Springer-Verlag : New York.

APPENDIX 1

Rock specimens, Davey Quadrangle

The following rock specimens are stored at the Department of Mines, Hobart. Rocks for which a thin section is available are marked (TS). Not all specimens have been referred to in the text of the report. The orientation implies that a mark exists on the rock, enabling geographic re-orientation of that specimen in the laboratory. The dip direction is the direction at right angles to the strike reading, in an anticlockwise direction. For example 120.73(T) is a dip of 73° towards 030°. The 'T' indicates that the mark is on an upwards facing surface, 'B' indicates that the mark is on a downwards facing surface. All direction values relate to true north.

Reg. No.	Sample No.	Orientation	AMG Ref.	Section	Description
76-443	PD 1		DN05061011	TS	Garnet biotite schist
76-444	PD 2	120.73 T	DN04401073	TS	
76-445	PD 3	190.15	DN04301069	TS	Albite biotite schist
76-446	PD 4	343.59	DN04301069		Folded layering
76-447	PD 5	355.55	DN04301069		Albite muscovite schist
76-448	PD 7	046.68	DN03551069	TS	Folds (F_2)
76-449	PD 8	253.64	DN03441062		Quartzite with mullions
76-450	PD 9		DN03101055	TS	Mica schist
76-451	PD10		DN03101055	TS	Albite schist
76-452	PD11		DN06710858		Very coarse to pebbly quartzite
76-453	PD12	245.75	DN03730891	TS	Garnet albite schist
76-454	PD13	219.66 B	DN03730891	TS	Mica schist
76-455	PD14		DN03730891		Garnet schist
76-456	PD15		DN03730891	TS	Garnet amphibolite
76-457	PD16		DN03730891	TS	Chlorite schist
76-458	PD17		DN03730891		Garnet amphibolite
76-459	PD18	254.82 B	DN03780896		Laminated quartzite and phyllite
76-460	PD19		DN03780896	TS	Fine grained chlorite schist
76-461	PD20		DN03770909	TS	Albite porphyroblasts
76-462	PD21		DN03790922	TS	Garnet schist
76-463	PD22	160.56	DN03790922	TS	Albite schist
76-464	PD23	200.80	DN03790922	TS	Coarse grained garnet schist
76-465	PD24		DN03790922	TS	Garnet
76-466	PD25	010.51	DN03920959	TS	Differentiated crenulation cleavage
76-467	PD26		DN08740827	TS	S_2 and S_3 in phyllite
76-468	PD27		DN08660835	TS	Three cleavages in phyllite
76-469	PD28		DN08830871		Garnetiferous phyllite
76-470	PD29	300.66 B	DN08830871	TS	Garnet, pre-S_2 in phyllite
76-471	PD31		DN08490967		Quartz-biotite schist
76-472	PD32		DN03930975	TS	Garnet schist
76-473	PD33		DN03880982	TS	Albite-chlorite schist

Appendix 1 (continued)

Reg. No.	Sample No.	Orientation	AMG Ref.	Section	Description
76-474	PD34		DN03860985	TS	Albite schist
76-475	PD35	001.49 T	DN03871001	TS	Quartzite
76-476	PD36		DN03871001	TS	Chlorite-albite schist
76-477	PD37		DN03931006		Chloritised garnet schist
76-478	PD38	352.51 B	DN03931006	TS	
76-479	PD39		DN03801042	TS	Garnet amphibolite
76-480	PD40	211.84 B	DN06380677	TS	Quartzite
76-481	PD41	232.58 B	DN06500684	TS	Quartzite
76-482	PD42	302.27 T	DN04710709		S_3 cleavage
76-483	PD43		DN03930777		Garnet schist
76-484	PD44		DN03930777	TS	Coarse garnet-muscovite schist
76-485	PD45		DN03930777	TS	Garnet-schist
76-486	PD46		DN04020787	TS	Albite schist
76-487	PD47		DN04020787	TS	Garnet-epidote-amphibolite schist
76-488	PD48		DN04020787	TS	Albite-biotite schist
76-489	PD49		DN03970801	TS	White garnet schist
76-490	PD50		DN03970824	TS	Garnetiferous quartzite
76-491	PD51		DN03630859	TS	Garnet-biotite-muscovite schist
76-492	PD52		DN07770768	TS	Consolidated beach material
76-493	DH 1		DN09060443	TS	Garnet amphibolite
76-494	DH 2		DN09000437	TS	Garnet amphibolite
76-495	DH 3		DN08880454	TS	Garnet-amphibolite-zoisite schist
76-496	DH 4		DN07940468	TS	Biotite-muscovite-quartz-albite schist
76-497	DH 5	184.26 T	DN09980592	TS	Quartzite
76-498	DH 6		DN09710686	TS	Garnet-mica schist
76-499	DH 7	018.48 T	DN09730694	TS	Garnet-mica schist
76-500	DH 8		DN10560745	TS	S_3 crenulation cleavage
76-501	DH 9		DN10990837	TS	Garnet-mica schist
76-502	DH10		DN12450872	TS	Garnet mullions
76-503	DH11		DN12830513	TS	Low-angle cleavage
76-504	DH12		DN12320613	TS	S_3 cleavage
76-505	DH13		DN12330652	TS	Laminated quartzite
76-506	DH14		DN12320658	TS	Dolerite
76-507	DH15		DN11950487	TS	Cleavage in F_2 folds
76-508	DH16		DN09670373	TS	Albite-mica-garnet schist
76-509	DH17		DN09670373	TS	Albite-biotite schist
76-510	SB 1	242.85 T	DM160975	TS	Green phyllite
76-511	SB 2	256.65 B	DM151978		F_2 S folds
76-512	SB 3	270.70 B	DM133971	TS	Quartz-mica schist
76-513	SB 4	175.70 T	DM168939		Quartz-schist
76-514	SB 5		DM155961	TS	Two crenulation cleavages in phyllite

Appendix 1 (continued)

Reg. No.	Sample No.	Orientation	AMG Ref.	Section	Description
76-515	SB 6	080.44 T	DM170989	TS	Cleavage in massive quartzite
76-516	SB 7		DM165983	TS	Green phyllite
77-190	BB 1	235.31 T	DN12801094	TS	Albite schist
77-191	BB 2		DN12801094	TS	Contact rocks in amphibolite
77-192	BB 3		DN12801094	TS	Contact rocks in schist
77-193	BB 4		DN12801094		Amphibolite
77-194	BB 5	294.20 T	DN12861103	TS	Coarse-grained garnet schist
77-195	BB 6		DN12731089	TS	Quartz-biotite schist and fold
77-196	BB 7		DN10831023	TS	Garnetiferous phyllite
77-197	BB 8		DN09390939	TS	Isoclinal fold - Whitehorse Creek (float)
77-198	BB 9	280.47 T	DN06890498	TS	Hinge region of D_2 fold
77-199	BB10		DN06660474	TS	Isoclinal folds
77-200	BB11	200.73 T	DN06580402	TS	
77-201	BB12		DN06500444	TS	Quartzite
77-202	BB13		DN06500444	TS	Biotite schist
77-7	CB 1	087.40 T	DN17140836	TS	
77-8	CB 2	281.27 T	DN17380610	TS	
77-9	CB 3	270.66 T	DN17570670	TS	Two late cleavages
77-10	CB 4		DN17570670	TS	S_2(?) cleavage
77-11A, B	CB 5		DN16240796	TS	F_1(?) fold and cleavage
77-12	CB 6	251.51 T	DN 16330869	TS	Banded schist
77-13	CB 7		DN16020911	TS	Albite schist
77-15	CB 9	100.35 T	DN15280757	TS	F_1 or F_2 fold
77-16	CB10	106.60 T	DN15730678	TS	Clastic dykes and S_2 cleavage
77-17	CB11	342.38 T	DN18020691	TS	Probable F_2 fold

I. C. CARTER, ACTING GOVERNMENT PRINTER, HOBART, TASMANIA

GEOLOGICAL SURVEY EXPLANATORY REPORT 91 DAVEY ISBN 0 7246 0507 X